# EXPERIMENTAL TECHNIQUES FOR THE STUDY OF LIQUID MONOPROPELLANT COMBUSTION

A Thesis

by

WILLIAM CHARLES WARREN

Submitted to the Office of Graduate Studies of
Texas A&M University
in partial fulfillment of the requirements for the degree of

MASTER OF SCIENCE

May 2012

Major Subject: Mechanical Engineering

Experimental Techniques for the Study of

Liquid Monopropellant Combustion

# EXPERIMENTAL TECHNIQUES FOR THE STUDY OF LIQUID MONOPROPELLANT COMBUSTION

A Thesis

by

WILLIAM CHARLES WARREN

Submitted to the Office of Graduate Studies of
Texas A&M University
in partial fulfillment of the requirements for the degree of

MASTER OF SCIENCE

Approved by:

| | |
|---|---|
| Chair of Committee, | Eric L. Petersen |
| Committee Members, | Adonios Karpetis |
| | Andrew Duggleby |
| Head of Department, | Jerald A. Caton |

May 2012

Major Subject: Mechanical Engineering

# ABSTRACT

Experimental Techniques for the Study of

Liquid Monopropellant Combustion. (May 2012)

William Charles Warren, B.S., The University of Alabama

Chair of Advisory Committee: Dr. Eric L. Petersen

Propellants based on hydroxylammonium nitrate (HAN) have shown promise as a hydrazine replacement because of their comparably low toxicity, low vapor pressure, high specific impulse and high density. Herein, the recent history of advanced monopropellant research is explored, and new experimental techniques are presented to investigate the combustion behavior of a potential hydrazine replacement propellant. Nitromethane, a widely available monopropellant with a recent resurgence in research, is utilized in the current study as a proof of concept for the newly designed equipment and as a step towards investigating more-advanced, HAN-based monopropellants.

A strand bomb facility capable of supporting testing at up to 340 atm was employed, and experiments were performed between 28 atm and 130 atm. Burning rate data for nitromethane are calculated from experiments and a power correlation is established as

$$r\ (\text{mm/s}) = 0.33[P(\text{MPa})]^{1.02}$$

A comparison with available literature reveals this correlation to be very much in agreement to other studies of nitromethane. Other physical characteristics of

nitromethane combustion are presented. Updates to the facility and new methods to examine the combustion of liquid propellant are described in detail. Special focus is given to procedures and safety information.

To Charles, Becky, Ben, and Maggie

# ACKNOWLEDGEMENTS

I offer many thanks to my committee chair, advisor, and professor, Dr. Eric Petersen; under his guidance, I have grown tremendously as a scientist and engineer. Thanks to my committee members, Dr. Adonios Karpetis and Dr. Andrew Duggleby for being supportive and accommodating throughout the process.

I also want to extend my gratitude to the Air Force Research Laboratory, the partnership with whom the research contracts the last two years have developed.

Great thanks are due to my colleagues in the Petersen Research Group at Texas A&M University for their openness and willingness to answer questions, lend a hand on experiments, and foster a wonderfully collaborative work environment.

Thanks most of all to my father and mother, Charles and Becky Warren, for their unfaltering support and helpful advice; to my brother Ben for being a golf partner, confidant, and co-pilot back and forth on the several thirteen hour drives between Texas and Alabama; and to Maggie, the dog, for always being there and never asking much.

# NOMENCLATURE

## ROMAN LETTERS

| | |
|---|---|
| a | Burning rate pre-exponential factor |
| AFRL | Air Force Research Laboratory |
| DEHAN | Diethylhydroxylammonium nitrate |
| EIL | Energetic Ionic Liquid |
| h | Specific enthalpy |
| $h^o_f$ | Enthalpy of formation |
| HAN | Hydroxylammonium nitrate |
| HEHN | Hydroxyethylhydrazinium nitrate |
| $I_{SP}$ | Specific impulse |
| N | Burning rate exponent |
| P | Pressure |
| r | Burning Rate |
| T | Temperature |
| t | Time |
| TEAN | Triethanolammonium nitrate |
| V | Volume |

GREEK LETTERS

| | |
|---|---|
| $\Delta$ | Finite change |
| $\rho$ | Density |
| $\sigma_p$ | Temperature sensitivity of burning rate |

SUBSCRIPTS

| | |
|---|---|
| AF | Adiabatic flame |
| r | Burning rate |
| rand | Random |
| tot | Total |

# TABLE OF CONTENTS

Page

# LIST OF FIGURES

# LIST OF TABLES

# 1. INTRODUCTION

Rockets deriving their thrust from the decomposition of chemicals are generally classified as either liquid propellants or solid propellants, or as hybrids which contain elements of both solid and liquid propellants. The category of liquid propellants includes bipropellants, in which a fuel and oxidizer are combined to combust or decompose, either hypergolically or via a separate ignition source, and monopropellants, which are substances as single chemicals or a homogeneous mixture of energetic chemicals which can decompose exothermically on their own to produce high-pressure gas.

Monopropellants find widespread use in propulsion applications for in-space reaction control system thrusters and to a lesser extent in gas generation for hydraulic pressure or mechanical systems, as in the Space Shuttle main engines (NASA, 1988). Of these in-space monopropellants, hydrazine is currently the most widely utilized, most often in a configuration with a platinum-group, metal-based catalyst bed. Over the years, a variety of monopropellants have been implemented in various roles, such as high-test hydrogen peroxide, nitromethane, ethylene oxide (Aerojet, 1958), and nitrous oxide have been used in addition to hydrazine (Sutton and Biblarz, 2001; Ward, 2010). In recent years, safer, more handleable monopropellants based on hydroxylammonium nitrate - commonly referred to as HAN - have also been explored for rocket propulsion as well as experimental applications such as liquid gun propellants.[1]

---

This thesis follows the style of *Combustion Science and Technology*.

## 1.1 Hydrazine Replacement

In the last two decades, there has been an increasing push to find replacements for hydrazine and hydrazine-derived monopropellants. Hydrazine presents stark dangers to human health and is therefore difficult and expensive to manufacture and handle. The dangers of hydrazine include high vapor toxicity as well as vapor pressure, unsafe thermal instability, a low autoignition temperature, and susceptibility to shock.

Monopropellants based on the energetic ionic-liquid (EIL) hydroxylammonium nitrate have shown promise as a potential partial hydrazine replacement in propulsion applications because HAN appears to address many of the weaknesses and concerns posed by hydrazine-based fuels. HAN-based propellants are generally distinguished by their low melting points, low-to-negligible vapor pressure, low toxicity, relatively high density, and good thermal stability (Hawkins et al., 2010).

HAN-based propellants are usually three-part mixtures: HAN, a fuel component, and a small amount of water. Fuels that have been used in combination with HAN in the past include hydroxyethylhydrazinium nitrate (HEHN, $HO\text{-}C_2H_4\text{-}NHNH_3{+}NO_3\text{-}$, $CH_9N_3O_4$), triethanolammonium nitrate (TEAN, $NH(C_2H_4OH)_3NO_3$, $C_2H_{16}N_2O_6$), and diethylhydroxylammonium nitrate (DEHAN, $(CH_3CH_3)HNOH{+}N03$) (Vosen, 1990; Jones et al., 2002; Mueller, 1997; Fortini et al., 2008). TEAN and DEHAN have found application in prototype liquid gun propellant systems designed by the US Army, respectively propellants LGP1846 and LGP 1898 (Jankovsky, 1996). Because of the

nature of the application of monopropellants as part of reaction control systems or gas generators for governmental and military spacecraft, much of the information concerning ionic-liquid fuel components is classified or at the very least sensitive under the International Traffic in Arms Regulations (ITAR) in the United States. The water component is used for three main purposes - lowering the viscosity of the fuel solution to accommodate better flowing conditions in a thruster application, improving the thermal stability of the monopropellant, and finally to lower the flame temperature (Sutton and Biblarz, 2001). This last point on flame temperature is vitally important, as currently many of the newer monopropellant blends burn at hotter temperatures than the sintering temperature of the more widely available platinum-group metal and ceramic-based catalysts, such as Shell-405 (Edwards, 2003). Research in materials engineering is currently underway to create and improve more robust catalyzing substances that can withstand the more rigorous demands of advanced monopropellants (Fokema and Torkelson, 2006; Fortini et al., 2008).

One potential non-EIL fuel which has found resurgence in research in recent years for use in monopropellant applications is nitromethane ($CH_3NO_2$), which is widely available and utilized currently in a range of combustion roles and industrial processes.

## 1.2 Overview of Study

The current study displays the development of techniques for the examination of liquid monopropellant combustion. Nitromethane was selected as the propellant for this

study as a step towards evaluating advanced, HAN-based monopropellants in future experiments. Equipment originally designed for the ignition of solid rocket propellant has been redesigned and repurposed for the current study. The facility in which the experiments took place is described in detail herein. Burning rate results and analysis, characteristic of the experimental setup, are demonstrated through a region of pressure ranging from 28 atm to 130 atm. The particular range was selected as it best typified the upper reaches of standard operating conditions for engines currently under development for both EIL-based and standard monopropellants.

Supplementary information in the form of appendices is provided at the conclusion of the text. These include a full experimental procedure, schematics for mechanical designs, materials lists, and a sample code for computer calculation.

# 2. BACKGROUND

## 2.1 Propellant for the Study

The ultimate goal of the new additions and modifications to the propellant laboratory is was the testing and evaluating of experimental advanced monopropellants, particularly those HAN-based monopropellants under development in recent years.

For the current study, nitromethane was utilized as a stand-in monopropellant for more-advanced monopropellants, especially those based on HAN. Nitromethane possesses very low toxicity, is relatively inexpensive, and is easily obtainable compared to other monopropellants like hydrazine or high-test hydrogen peroxide, and it can be handled safely under normal laboratory conditions.

## 2.2 Nitromethane

Nitromethane is a clear, colorless liquid at room temperature, and is used in a variety of combustion applications: as a monopropellant, a fuel in mixture with methanol for “Top Fuel” drag racing, and an additive to other fuels to improve performance in small combustion chambers.

For many years, nitromethane has been discussed as a monopropellant for use in spaceflight propulsion applications. However, after an initial period of research interest following the Second World War, priority shifted towards hydrazine-based fuels as a

result of their easier ignition while retaining acceptable performance values. Most recently, efforts have been made to utilize nitromethane in micro- and meso-scale propulsion systems. The energy density of nitromethane coupled with its good thermal stability and very low toxicity make it ideal for the laboratory testing of small-scale propulsion devices. Recently, a group of researchers from The Pennsylvania State University as well as Princeton University have developed a working prototype of a meso/micro-scale liquid-monopropellant thruster utilizing nitromethane as the propellant (Yetter et al., 2007). It should be noted that this thruster achieves initial ignition and sustains the combustion during the start-up transient with an addition of small amounts of a methane/oxygen mixture into the combustion chamber. Regardless, at steady state the combustor operates completely via nitromethane burning without the presence of separate oxidizer.

### 2.2.1 Comparison to Other Monopropellants

Nitromethane, as with HAN-based monopropellants, offers distinct advantages over hydrazine as a viable monopropellant for most applications and especially for spacecraft propulsion. Nitromethane is cheaper, more widely produced, less toxic, easier stored and handled, denser, and with a higher specific impulse than hydrazine. The vapor pressure of nitromethane at room temperature is 36 mmHg (CRC, 1962), slightly higher than hydrazine at 14.4 mmHg at the same temperature (OEHHA, 2000). One drawback of nitromethane is a very high flame temperature when compared to other rocket

monopropellants; 2790 K compared to 1394 K for hydrazine, and 2157 K for a 44.5/44.5/11 wt% HAN-HEHN monopropellant (Fortini et al., 2008). However, the drawbacks of this higher flame temperature are mitigated somewhat by the lack of a need for a catalyst to ignite nitromethane and sustain combustion; therefore, material restraints are less so for nitromethane than for a propellant needing a catalyst. Table 1 gives a clearer juxtaposition of selected material and performance values of nitromethane as compared to hydrazine. Flame temperature and specific impulse for this comparison were calculated utilizing the Chemical Equilibrium with Applications (CEA) code from NASA Glenn, at conditions of 1000 psia chamber pressure and a 50:1 expansion ratio.

**TABLE 1. Selected performance values and material properties of monopropellant nitromethane and hydrazine**

| | Nitromethane $CH_3NO_2$ | Hydrazine $N_2H_4$ |
|---|---|---|
| Molecular Weight | 61.04 g/mol | 32.05 g/mol |
| Density – ρ | 1.127 g/cm³ | 1.013 g/cm³ |
| Specific Impulse – $I_{SP}$ | 276 s | 234 s |
| Density Impulse – $\rho I_{SP}$ | 311 | 237 |
| Flame Temperature – $T_{FLAME}$ | 2188°C | 1121°C |
| Toxicity - $LD_{50}$(rat) | 940 mg/kg | 60 mg/kg |

The calculations from CEA line up with published values for nitromethane and hydrazine. Czysz and Bruno (2006) also list $I_{SP}$ and $\rho I_{SP}$ values for the two as 273 and 308 s for nitromethane, and 218 and 219 s for hydrazine. Fortini et al. (2008) corresponds closer to the calculations herein as it lists the $I_{SP}$ for hydrazine at 234 sec.

### 2.2.2 Safety for Nitromethane

Nitromethane is not, however, without other drawbacks. Though relatively stable when compared to other liquid fuels, monopropellants or otherwise, accidents can and have occurred. Perhaps the largest of these took place near Mt. Pulaski, Illinois in 1958, in which a tanker car filled with 10,000 gallons of nitromethane detonated, blasting a crater 100 feet in diameter and 36 feet deep, killing two people and wounding four others (Interstate Commerce Commission, 1958). This and other smaller incidents led to the conclusion that nitromethane is susceptible to detonation upon large shocks, and must be handled and stored accordingly.

As identified by Dow Chemical Company (2011), three unsafe conditions must be avoided when handling nitromethane: severe shock, above that equivalent to a number eight blasting cap; rapid compression without adequate heat loss; and heating above its critical point in confined spaces. Other safety information and precautions taken in the Propellant Laboratory can be found in Appendix A.

### 2.2.3 Nitromethane Chemistry

Calculated utilizing the STANJAN chemical equilibrium code and with starting conditions at 298 K and 1000 psia, the global chemical reaction for the decomposition of nitromethane in stoichiometric oxygen is as follows:

$$CH_3NO_2 + 0.75\ O_2 \rightarrow 1.5\ H_2O + CO_2 + 0.5\ N_2 \quad (1)$$

However, in the absence of an outside oxidizer, as would be in the case in a monopropellant system, nitromethane decomposition is less complete, resulting in the following, as calculated utilizing the STANJAN chemical equilibrium code and with starting conditions at 298 K and 1000 psia:

$$CH_3NO_2 \rightarrow 0.837H_2O + 0.157CO_2 + 0.842CO + 0.659\ H_2 + 0.499\ N_2 + 0.005\ OH \quad (2)$$

Monopropellant combustion of nitromethane occurs at 39% oxygen lean conditions. From Equation 2, the flame temperature can be calculated using an enthalpy balance at equilibrium. Balancing the enthalpy for the reactants and the products can be written as:

$$\sum_i \left[N_i h_i\right]_{react} = \sum_j \left[N_j h_j\right]_{prod} \quad (3)$$

where h is specific enthalpy in units of KJ/mol, and N is the number of moles of a particular species in the reaction. Specific enthalpy can be expanded into its components as follows for Equation 4:

$$\sum_i N_i[(h_i(T) - h(298K)) + h^o_{f,i}]_{react} = \sum_j N_j[(h_j(T) - h(298K)) + h^o_{f,j}]_{prod} \quad (4)$$

where $h_i(T)$ is the sensible enthalpy as a function of temperature with regards to a reference condition at 298 K, and $h^o_{f,i}$ is the enthalpy of formation for a given species,

both on a molar basis. Using the NASA polynomials to calculate *h(t)* and assuming that the temperature at the enthalpy balance is the adiabatic flame temperature ($T_{AF}$), it can be calculated in this way that for nitromethane monopropellant combustion $T_{AF}$=2790 K.

Also necessary to the design and operation of a rocket motor is the ability to model the combustion process by means of chemical kinetics. The current study does not undertake an investigation into the chemical kinetics of nitromethane ignition and combustion, but prior studies have built foundational models for this purpose, including Boyer and Kuo (1999), Kelzenberg et al. (1999), Yetter and Rabitz (1989), and Boyer (2005). As identified by Yetter et al. (2007), the following are the most important elementary reactions with regard to the combustion of nitromethane:

$$CH_3NO_2 + M \rightarrow CH_3 + NO_2 + M \quad (5)$$

$$CH_3 + NO_2 \rightarrow CH_3O + NO \quad (6)$$

$$CH_3O + M \rightarrow CH_2O + H + M \quad (7)$$

$$H + NO_2 \rightarrow NO + OH \quad (8)$$

$$OH + CH_3NO_2 \rightarrow H_2O + CH_2NO_2 \quad (9)$$

$$CH_2NO_2 + M \rightarrow CH_2O + NO + M \quad (10)$$

$$CH_2O + OH \rightarrow HCO + H_2O \quad (11)$$

$$HCO + M \rightarrow CO + H + M \quad (12)$$

$$CO + OH \rightarrow CO_2 + H \quad (13)$$

The same study noted the lack of molecular oxygen as the main source of radicals at low pressure; rather, pressure-dependent dissociation reactions reign. As discussed in Section

6, this hypothesis comes to confirmation as the ignition of nitromethane becomes increasingly difficult at the pressure regime below 400-500 psia.

Boyer (2005) noted that, "the gasification rate of the condensed phase is determined by conductive heat feedback from the gas phase," and identified the most temperature-sensitive elementary reactions, as these would have the most effect on the gasification rate and subsequent combusting of nitromethane vapor. These reactions at 3 MPa were established to be:

$$N + CO_2 \rightarrow NO + CO \quad (14)$$

$$NH + OH \rightarrow HNO + H \quad (15)$$

$$HNO + H \rightarrow H_2 + NO \quad (16)$$

$$HNO + NO \rightarrow N_2O + OH \quad (17)$$

$$CH_3 + NO_2 \rightarrow CH_3O + NO \quad (18)$$

The propellant laboratory at Texas A&M University has not conducted chemical kinetics model calculations for nitromethane, but plans to pursue such a model for this and other rocket monopropellants, especially HAN-based EILs. Preliminary steps have been taken and are currently underway to employ aerosol shock-tube methods to perform gas-phase kinetics measurements of liquid monopropellants.

## 2.3 Burning Rate

Design and operation of rocket engines depends heavily on the internal ballistics of the propellant utilized. Because solid propellants are generally employed in

unthrottlable, single-use motors the burning rate, or regression rate, is one of the most important design parameters for solid propellant motors. However, knowledge of the burning rate is also important to the understanding of the combustion behavior of liquid propellants. Empirical observation yields the burning rates rate, *r*, which is defined as

$$r = aP^n \tag{19}$$

where $a$ is pre-exponential factor dependent in part on initial propellant temperature, $P$ is the chamber pressure, and $n$ is the burning rate exponent which is independent of temperature and is instead a descriptor of the effect of pressure (Sutton and Biblarz, 2001).

Burning rate can be temperature dependent; generally there is a positive correlation between the pre-burn temperature of the propellant and the burning rate. Sutton and Biblarz (2001) demonstrate that this temperature sensitivity of burning rate, $\sigma_p$, can be shown in terms of temperature coefficients as follows:

$$\sigma_p = \left( \frac{\delta \ln r}{\delta T} \right)_P = \left( \frac{\delta \ln(aP^n)}{\delta T} \right)_P = \frac{1}{a} \frac{da}{dT} \tag{20}$$

The temperature sensitivity of burning rate is dependent primarily on the composition of the propellant and the combustion mechanism of the propellant.

## 2.4 Combustion Methods

A result of the low vapor pressure of HAN-based propellants is that it often prevents full gas-phase ignition (Alfano et al., 2009). For this reason as well as the

mechanisms of most monopropellant rocket engines, the HAN-based propellants will be introduced as liquid sprays in real spacecraft propulsion applications (Fokema and Torkelson, 2008). Both pools and sprays of propellant have been successfully ignited in laboratory settings, yielding a variety of ignition techniques, including resonant lasers (Alfano et al., 2009), electrical arc (Vosen, 1990), as well as heated nichrome wire (Smiglak et al., 2006; Chang et al., 2000).

Despite the high vapor pressure of nitromethane over energetic ionic liquid propellants, it remains important for the establishment of future experiments that nitromethane be ignited in the same configuration designed within the constraints of a low vapor pressure propellant. Nitromethane finds widespread use in a variety of combustion applications, and can sustain combustion in a range of conditions. However, to achieve the accuracy of measurement required to understand certain fundamental combustion characteristics such as linear burning rate, a strand burner device proves reliable.

Indeed, several groups in the past have utilized strand burners with nitromethane to derive burning rate data. Most recently, Boyer and colleagues ignited nitromethane at pressures from 3 MPa to 170 MPa in both static and fed systems (2005, 1999). Burning rates in these studies at The Pennsylvania State University established the following burning rates according to Equation 19 in the three pressure regimes using a quartz tube method as well as an ultra-high pressure strand burner (UHPSB):

$$r_b(\text{mm/s}) = 0.173[P(\text{MPa})]^{1.17} \text{ (for } 3<P\leq 15 \text{ MPa)} \quad (21)$$

$$r_b(\text{mm/s}) = 0.009[P(\text{MPa})]^{2.33} \text{ (for } 15<P\leq 70 \text{ MPa)} \quad (22)$$

$$r_b(\text{mm/s}) = 4.153[P(\text{MPa})]^{0.86} \text{ (for } 70<P\leq 170 \text{ MPa)} \quad (23)$$

Utilizing a liquid propellant strand burner (LPSB) method similar to that in the current study, Boyer and Kuo (1999) as well as Boyer (2005) discovered a burning rate of

$$r_b(\text{mm/s}) = 0..299[P(\text{MPa})]^{1.03} \text{ (for } 2.5<P\leq 15 \text{ MPa)} \quad (24)$$

In 1999, researchers in Germany established a burning rate as well as a simplistic model of nitromethane combustion under strand burner conditions (Kelzenberg et al., 1999). In the late 1970s in Moscow, Raikova and colleagues (1977) conducted burning rate studies between 6.5 and 30 MPa. Soon after World War II, as nitromethane was being widely investigated as a potential mono- and bipropellant, Rice and Cole (1953) with Naval Ordnance (NAVORD) conducted experiments up to 25,000 psig (172 MPa). The rates from these burning rates from the literature are compared in Figure 1.

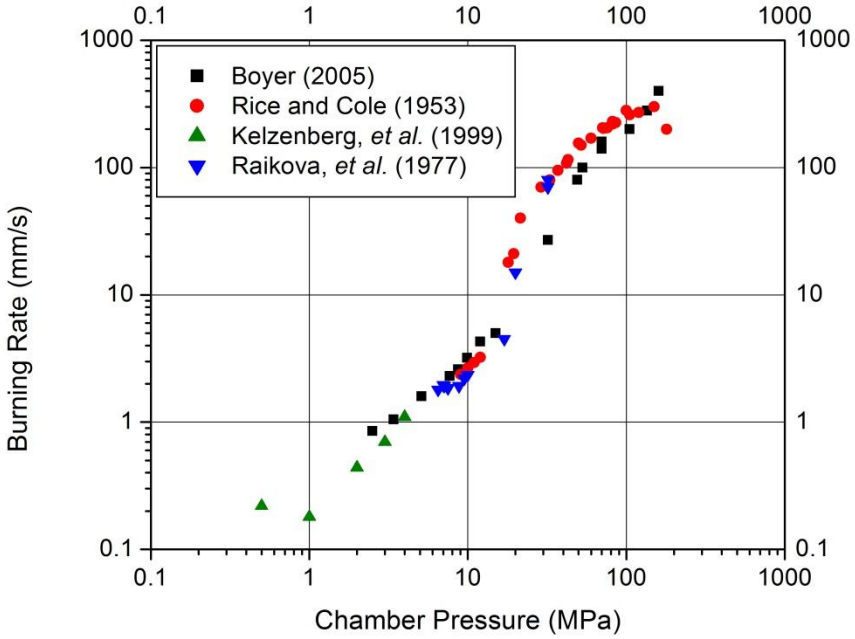


**Figure 1. Burning Rate Measurements for studies from Boyer (2005), Rice and Cole (1953), Kelzenberg et al. (1999), and Raikova et al. (1977)**

Recently, efforts have been made to explore additives to nitromethane in an effort in enhance its burning rate for use in high-speed propulsion systems. A joint research effort between The Pennsylvania State University and Princeton University has investigated the use of colloidal particles of graphene or metal hydroxides as suspended additives in nitromethane (Sabourin et al., 2009). This study found that these carbon or metal additives increase the burning rate for nitromethane as well as make the propellant less pressure-dependent than the rate in the same region from Equation 21, lowering the exponential factor $n$ to 0.81 while raising the pre-exponential factor $a$ to 0.475.

# 3. EXPERIMENT

## 3.1 Propellant Laboratory

Located within the Turbomachinery Laboratory on the campus of Texas A&M University, the Propellant Laboratory (floorplan in Figure 2) is one of two laboratory spaces dedicated to combustion research. The Propellant Laboratory possesses the equipment and resources to study the burning behavior of both solid and liquid propellants, generally for rocket applications.

Safety of the researchers and technicians is of vital importance in the Propellant Lab, and there exist many layers of safety equipment and protocol designed to all but eliminate hazards to personnel. For example, the floor in the laboratory is a multi-feet deep floating concrete slab coated with an electro-static dissipating (ESD) epoxy, drastically reducing the danger of accidental ignition of a propellant by errant static charges (Kreitz, 2010). Reinforced concrete blast walls and steel blast doors isolate the test cell whenever the strand bomb is pressurized. Ventilation for the propellant lab is fed into the main exhaust system for the building and when activated evacuates and recycles the air in the lab every 90 seconds or so. In case of emergency, fire suppression equipment includes a sodium chloride powder extinguisher for metal fires and those involving strong solid propellant oxidizers, two carbon-dioxide extinguishers for most other flames, and finally a building-wide sprinkler system.

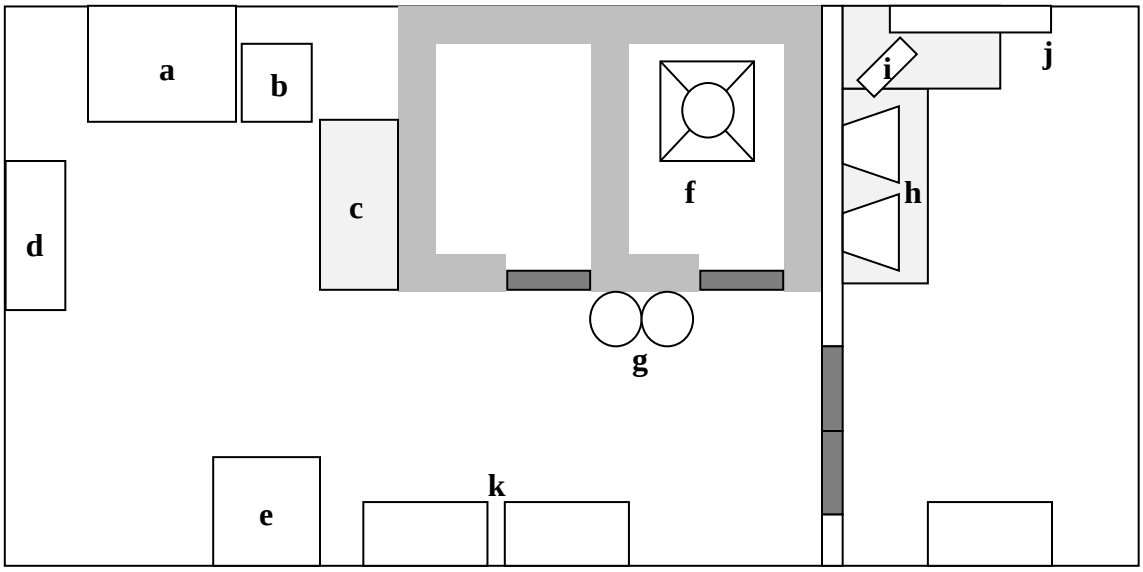


**Figure 2. Floorplan of Propellant Lab: (a) fume hood, (b) flammable waste bin, (c) work bench, (d) flammable fuels cabinet, (e) explosives magazine, (f) liquid propellant test cell with strand burner surrounded by reinforced blast walls and secured with blast door, (g) pressurant gas manifold, (h) DAQ computers, (i) control panel, (j) video monitoring screens, (k) storage**

The pressurized propellant burning apparatus is housed within an 8'×8' concrete cell, secured to a floating concrete slab, surrounded by reinforced concrete walls, and secured with a 1.5-inch steel blast door. The cell can be monitored remotely using a series of security cameras installed at various angles within the laboratory, viewable in the control room. The cameras serve a dual purpose: to ensure no personnel are present in a dangerous area during high-pressure experiments, as well remotely monitoring the test apparatus in case of an equipment failure. Figure 3 shows the schematic layout of the experimental equipment.

## 3.2 Strand Burner

As presented by Carro (2001), the strand bomb in which the experiments were performed has internal dimensions of a 3.70-inch diameter, 8.0-inch long steel cylinder with three optical ports around the lower midsection; an orifice for insertion of the burner plug on the underside of the bomb; and an inlet/outlet orifice connected to the inert gas pressurization line and exhaust line. A photograph of the bomb is presented in Figure 4. All exposed surfaces are coated with SS316 using a plasma spray. Each of the side optical ports is comprised of a 1.5-inch thick sapphire window with appropriate locking and sealing apparatuses. One of the side ports is used for acquiring visible, broadband light emission by use of a photodiode. The reading from the photodiode is one of the two indicators of ignition within the bomb; the other is a simultaneous spike in the pressure reading by way of an Omegadyne 7.5-kpsi pressure transducer attached to the top of the bomb. A second side port is reserved for the Ocean Optics USB2000 fiber optic spectrometer. The third, front-facing optical port can be used for remote visual inspection of the burning process, with a video camera.

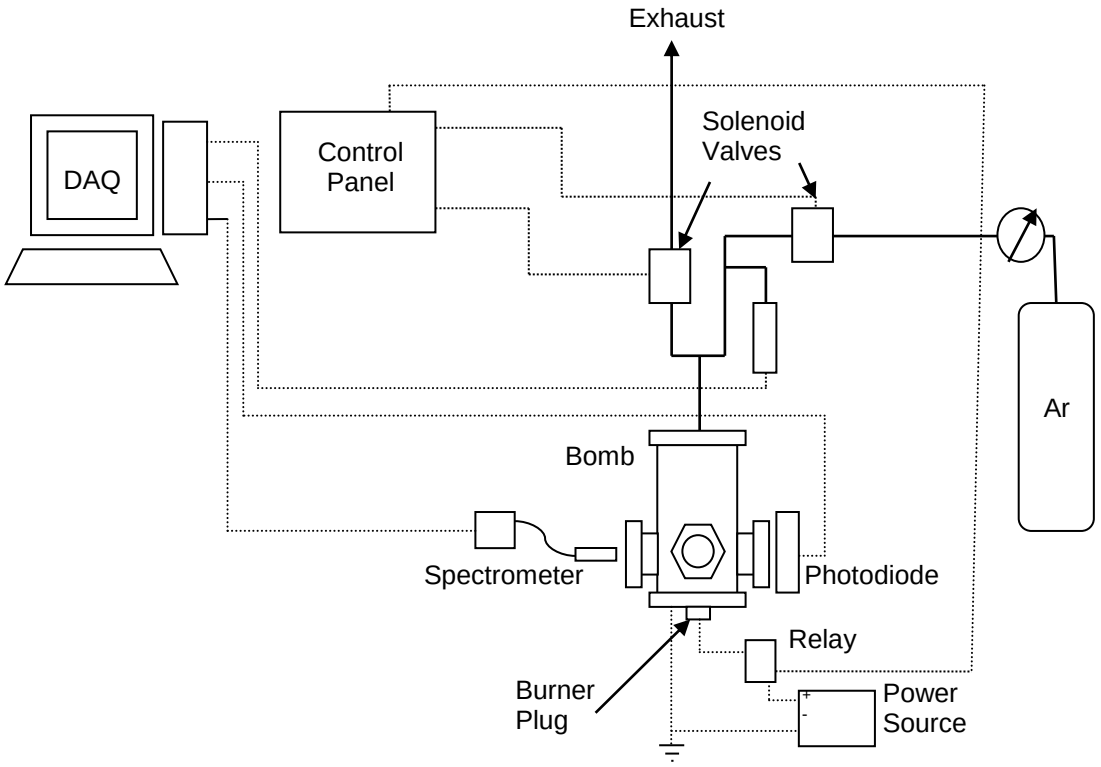


**Figure 3. Schematic of the control system for the strand bomb apparatus used to burn the monopropellant samples.**

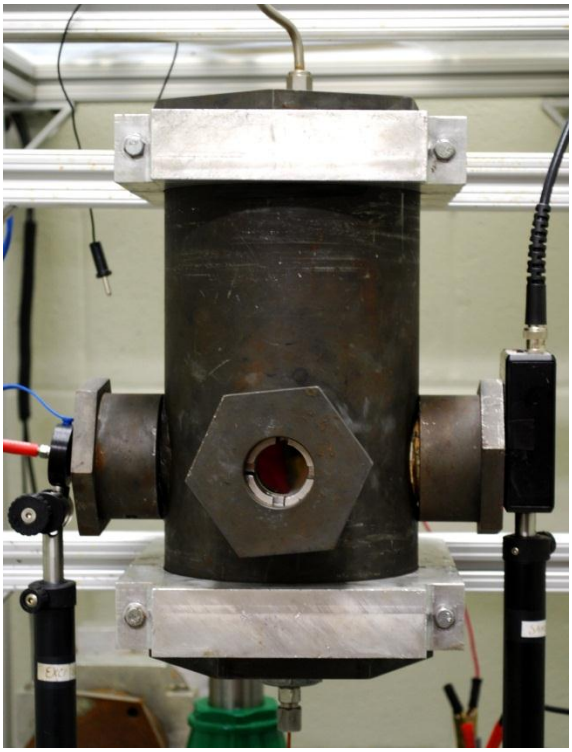

**Figure 4. Photograph of Strand Burner in test configuration. Components are as follows: (1) inserted burner bolt; (2) photodiode; (3) spectrometer lens; (4) optical port; (5) steel bomb casing; (6) fill/exhaust line**

A plug used to hold the monopropellant sample was specially machined for the present study from a 1.5-inch head, 3-inch long, fully threaded, zinc-coated, 1-inch steel bolt. Figure 5 shows a detail view of the sample holder. An inch of the bolt closest to the head remained threaded, to secure the bolt to the underside of the bomb, with O-rings attached and sealant applied to establish an effective seal. A hole, 0.125 inch in diameter, was drilled through the bolt lengthwise to accommodate an insulated, single-strand copper wire, which acted as the positive lead. A small eyelet was installed opposite the propellant cavity to secure a connection for the negative lead. The bolt and

bomb together constituted a grounded lead. The bomb was connected to the negative port in the power supply, and the entire apparatus was grounded. The cavity in which the propellant is placed is a 0.358-inch diameter hole drilled 0.375 inches deep and situated halfway in between the two leads. More-detailed dimensions for the bolt design and plans for manufacture can be found in Appendix C.

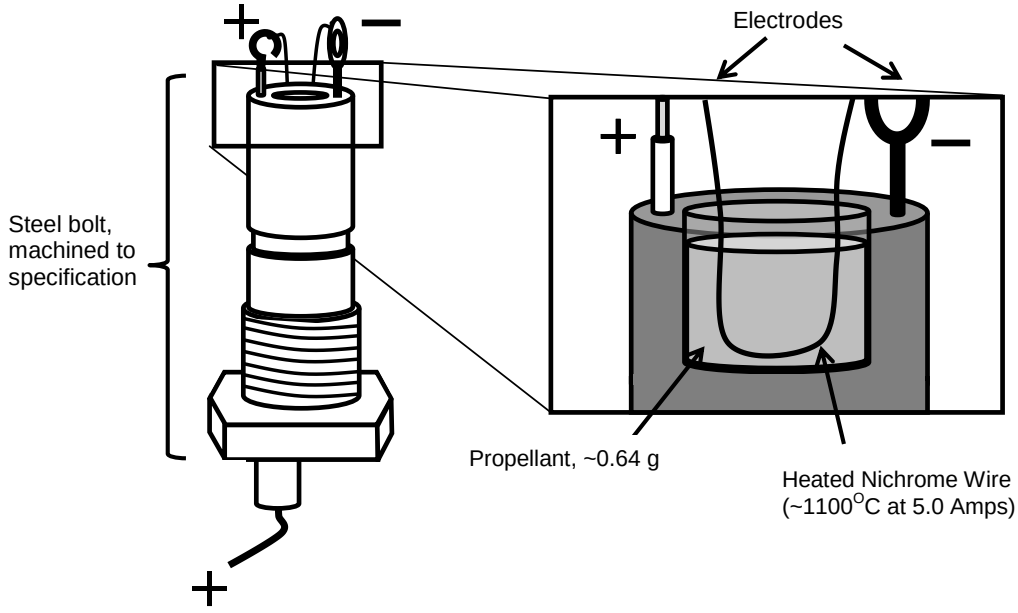


**Figure 5. Burner Plug, secured in the bottom of the strand burner, connected to a power source. Propellant is placed in the central cavity, which measures 0.358 inches in diameter and 0.375 inches deep.**

## 3.3 Control Room

Located adjacent to the propellant laboratory main room, the control room is protected from the high-pressure experiments by a reinforced-concrete blast wall. All

data acquisition (DAQ) software and controls necessary for performing a burning run are located within the control room. Figure 6 shows the two DAQ computers and the control panel, the primary electronic connections within the control room, and the four remote video monitoring viewscreens.


**Figure 6. Control Room: (a) DAQ computers, (b) control panel, (c) video monitors, (d) port for cables passing between test cell and control room**

One of the DAQ computers is reserved for the spectroscopic software package OceanOptics USB2000 and the second computer for oscilloscope software GageScope, which acquires and stores signals from the pressure transducers and photodiode. Data

analysis is performed on these computers or on separate, dedicated computers within the Turbomachinery Laboratory. This analysis utilizes Microsoft Excel to create and store large data files created by the DAQ software, while Origin 8.1 from OriginLab is used for data smoothing and plotting of experimental results.

## 3.4 Procedure

### 3.4.1 Safety

Establishment of safety protocols for researchers stands as the single most important aspect in the development of new experimental techniques for burning liquid propellants. Despite the dramatic improvements in safety and handleability of advanced monopropellants compared with hydrazine-based propellants, the new chemicals still present hazards that must be addressed.

Many of the advanced propellants have extremely low vapor pressures, but the risk of skin or eye exposure through splash or other incidental contact is solved through appropriate safety equipment. When handling propellants, researchers wear nitrile or neoprene gloves, full face respirators, long sleeves, and long pants. Specifics and supplier model numbers of the safety equipment utilized can be found in Appendices A and E.

To prevent any unexpected passers-by through the propellant laboratory, a bright warning light is prominently displayed on the outside of the entrance way to the

laboratory along with a corresponding sign which reads “High Pressure Experiment in Progress.”

### 3.4.2 Burning and Cleaning

Heating of the propellant in the cavity is achieved by coursing current through an AWG 30 gauge nickel chromium wire connected between the two leads at the top of the bolt and suspended into the propellant cavity. This configuration achieves a near-uniform heating of the entire propellant sample prior to ignition, giving burning rates a more realistic profile as opposed to quiescent pool fires of cool propellant. For the majority of tests in the present study, a current of 5 Amps was applied to the strand burner ignition circuit, heating the wire to approximately $1100^{O}$ C in the process. The circuit is completed manually with a remotely controlled relay switch, and current is run as long as the experiment is completed satisfactorily. Depending on the time for the propellant to commence burning, this current flow generally lasts for approximately ten seconds.

The temperature of the wire is calculated from known conditions of nickel chromium alloy at the given wire gauge and length. Nickel chromium 60 (or Nichrome A) exhibits resistivity of 6.5 Ohms/foot and a melting point of roughly $1350^{O}$ C. Based upon visual inspection of the wire while flowing a current of 5 Amps, it is noted that the wire rapidly reaches a maximum temperature and melts at some point along the middle of the wire, breaking the circuit in approximately 3 seconds. As most tests lead to the

ignition of the propellant in roughly 2.5 seconds, it is conjectured that the wire heats to very near the melting temperature at the point of ignition, most likely 1100±50$^{O}$ C. Figure 7 shows the obvious difference in visible radiation as the nichrome wire is fed current at various current levels. Once the combustion event for nitromethane begins, the burning propellant rapidly approaches its own flame temperature of over 2000$^{O}$ C, further disintegrating the wire. As such, it is established that once initial ignition occurs, the propellant is fully self-sustaining.

**Figure 7. Nichrome wire at (a) 2.5, (b) 3.5, and (c) 5.0 Amps. The last setting was utilized in all experiments presented in this study.**

The full, expanded experimental procedure can be found in Appendix B. An abbreviated procedure for an individual experiment is as follows. The bolt is cleaned with acetone and allowed to dry. A nickel chromium wire is wrapped around each of the

leads and suspended as far into the propellant cavity as possible without touching the side of the cavity. A small amount of propellant, roughly 0.65 grams, is measured out and weighed, then inserted into the burner bolt cavity (Figure 5). The strand bomb is then remotely purged with argon, and the bolt is secured to the underside. Figure 8 shows the pressurant manifold for the supply of high-pressure argon and AR/$O_2$ mixture.


**Figure 8. Pressurant manifold with high-pressure gas. Also shown is the secured blast door to the right as well as safety warning light discussed in Section 3.4.1.**

The bomb is then purged again with the inert gas and exhausted to remove any remnant non-inert gases. The bomb is then pressurized to the desired initial pressure. Following this setup, a final check is made to ensure the data acquisition software is running and the sensors are responding. The ignition switch is then depressed, closing a

circuit by means of a relay and allowing the 3.5 Amps of current to flow through the device. The current is delivered until several seconds after it is clear that combustion has ended. After the burning is complete, the system is exhausted, purged, and exhausted a second time. The bolt is then removed. Any unburned propellant is weighed; the difference between the initial weight of propellant and the final weight is calculated to be the amount burned in the experiment. These data are used with the known diameter of the cavity and the measured burning time described below to calculate burning rate. The bolt is then thoroughly cleaned and another experimental can be set up.

### 3.4.3 Calculations

Burning rate, as defined by the current study is linearized as

$$r = \frac{\Delta x}{\Delta t}$$

where $\Delta x$ is the linear length of a strand of propellant (when using a solid propellant), and $\Delta t$ is the elapsed burning time as calculated below. For a liquid monopropellant, the length $\Delta x$ is calculated from the amount of propellant burned in the experiment, the known surface area of the 0.358-inch diameter propellant cavity, and the known density of the propellant, in this case nitromethane with a density of 1.127 g/cm$^3$. As shown in Equation 25, $\Delta x$ is therefore calculated as

$$\Delta x = \frac{\left(\frac{m_p}{\rho}\right)}{\left(\frac{d^2}{4}\pi\right)} \tag{25}$$

where $m_p$ is the mass of the propellant sample, $\rho$ is the propellant density, and $d$ is the diameter of the propellant cavity.

For each experimental run, ASCII-format data files are created of voltage versus time for the pressure readings at a 1-kHz sampling rate from the 7.5-kpsi transducer. Raw data from GageScope (a screen-shot of which can be found in Appendix D) is processed via Origin 6.1, and the burn time of a particular run is calculated graphically, as shown in Figure 9. The point of ignition is defined as the intersection of the path of the steepest slope of the initial pressure rise with the initial baseline pressure before ignition. The end of combustion is calculated similarly, as the intersection of the steepest path of the slope with a horizontal line at the peak pressure reading. As is shown in Figure 9, there was typically some rounding at the top of the pressure curve. Based upon visual inspection of the behavior with which the propellant burns at lower pressures, this rounding is attributed to residual pressure effects within the strand bomb and is not considered part of the combustion event. The total burning time ($\Delta t$) is then defined as the time between the point of ignition and the end of combustion, or point of extinguishment.

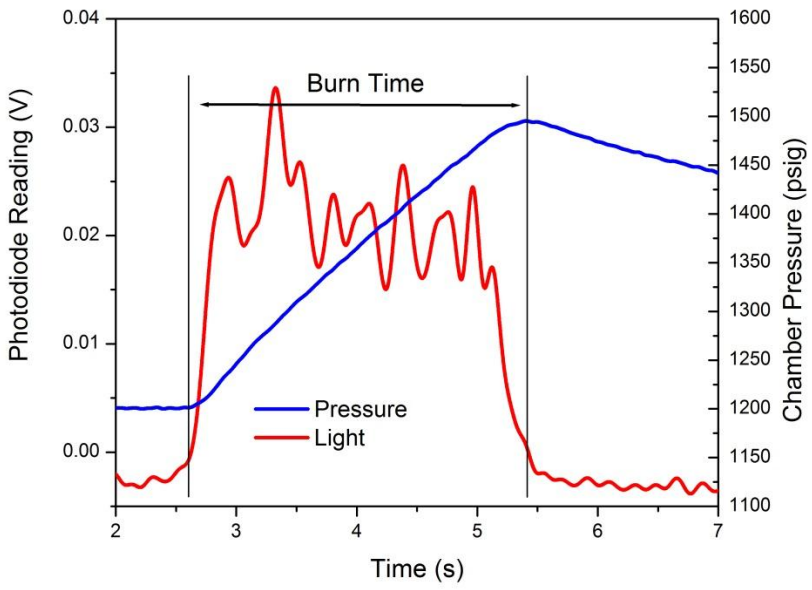


**Figure 9. Method for calculating the time of propellant burning duration. Burning time is defined as the period between the ignition event and extinguishment.**

Though all efforts were made to ensure precision and accuracy with these experimental techniques, there was unavoidable uncertainty which must be accounted. In general, raw data collected in experiments must be processed through several steps of calculation, each step containing an intrinsic uncertainty. For example, Equation 26 for the burning rate can be rewritten with all of its component parts as:

$$r = \frac{\Delta x}{\Delta t} = \frac{\left( \frac{\left( \frac{m_p}{\rho} \right)}{\left( \frac{d^2}{4} \pi \right)} \right)}{\Delta t} \tag{26}$$

Based upon this study and prior experiments with the same equipment, it is assumed that the uncertainty for the individual components of Equation 25 are as follows: $u_{mp} = \pm 0.01$ g from scale reading; $u_{rho} = \pm 0.01$ g/cm$^3$, from non-uniformity of manufacture on the supplier end; $u_d = \pm 0.001$ in, from the manufacture of the propellant cavity; and $u_{\Delta t} = \pm 0.05$ s. Propagation of error for the overall system is tracked using the root-sum-squared method for calculation of uncertainty as proposed by Moffat (1982):

$$U_r = \sqrt{\sum_{i=1}^{n} \left[ \frac{\partial r(x_i)}{\partial x_i} u_i \right]^2} \tag{27}$$

where $U_r$ is the uncertainty due to the experimental system, and $r(x_i)$ is burning rate as a function of its component variables. Then for the percent error of a system, where r is defined in Equation 26, the calculation becomes:

$$\frac{U_r}{r} = \sqrt{\left[ \left( \frac{u_{m_p}}{m_p} \right)^2 + \left( \frac{u_\rho}{\rho} \right)^2 + \left( 2\frac{u_d}{d} \right)^2 + \left( \frac{u_{\Delta t}}{\Delta t} \right)^2 \right]} \tag{28}$$

For the burning rate uncertainty for Equation 28, an average error of 2.6 percent is achieved across the range of pressures in this study. However, because of other potential minor non-idealities such as depth of the igniter wire, or fluctuations in ambient temperature, or aberrant pressure effects with the strand bomb, systemic uncertainty is coupled with an assumption of a random uncertainty of 5%. Equation 29 below shows the sum-of-squares method for the coupling of systemic and random uncertainty:

$$U_{r,tot} = \sqrt{U_r^2 + U_{r,rand}^2} \tag{29}$$

where $U_r$ is the uncertainty due to the system and $U_{r,rand}$ is random uncertainty of 5%, and $U_{r,tot}$ is the total uncertainty for a given calculation of burning rate.

# 4. RESULTS

## 4.1 Physical Characteristics of Propellant Flames

When burned utilizing the burner plug configuration under air at atmospheric pressure, all tested propellants burn with a low, stable flame. Visual inspection of propellant pool fires in the current configuration under atmospheric pressure shows a low, weak flame with minimal surface instability. Figure 10 shows an EIL monopropellant just before ignition as the nickel chromium wire heats and during burning while the flame is at its peak, and Figure 11 shows the same with nitromethane as the fuel.

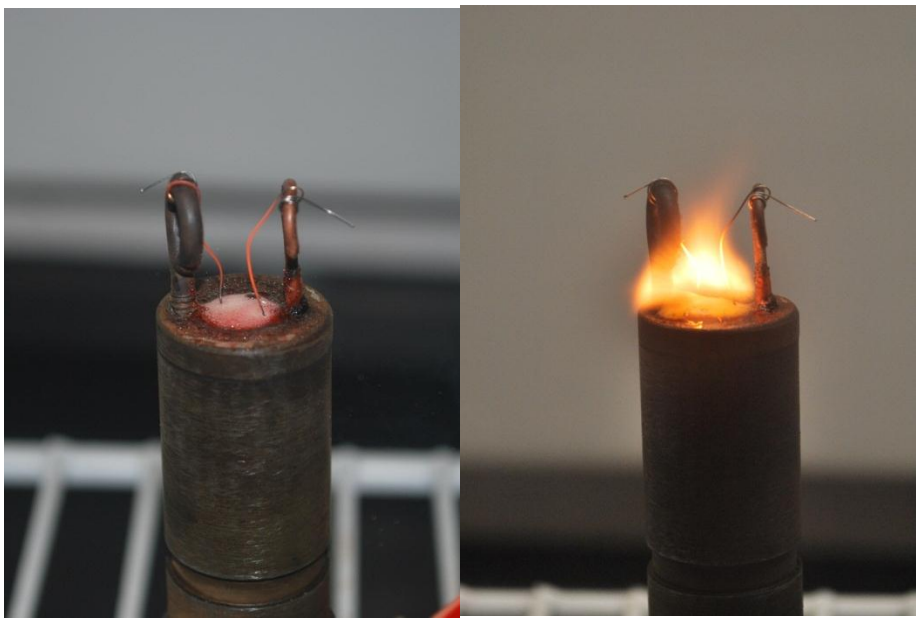

**Figure 10. (a) EIL monopropellant in air at 1 atm just before ignition, and (b) at the peak of the combustion process**

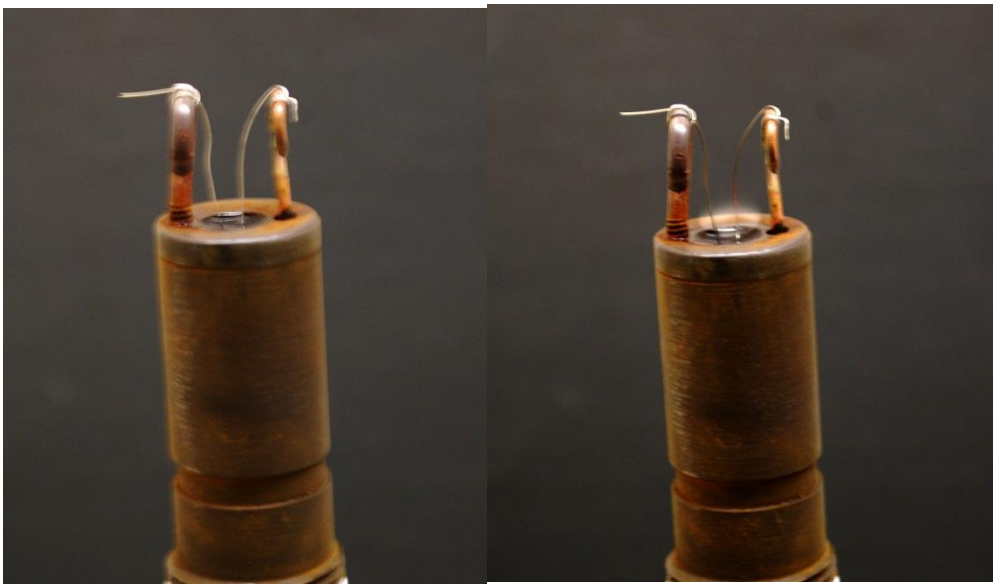

**Figure 11. (a) Nitromethane in air at 1 atm just before ignition, and (b) at the peak of the combustion process. Note the pale, weak flame above the propellant cavity compared to Figs 12 and 13.**

However, under very high pressures in the strand burner, propellants display much more intense, violent combustion characteristics consistent with their role as monopropellants for rocket propulsion applications. Figure 12 provides a look inside one of the optical ports of the strand bomb at 418 psig. The comparison between Figure 11b and Figure 12 clearly demonstrates the intensification of the nitromethane flame from 14.7 psia to 418 psig, and further from Figure 12 to Figure 13 at 1024 psig.

**Figure 12. Nitromethane flame at 418 psig. Dramatic increase in flame intensity from Figure 11b is evident.**

**Figure 13. Nitromethane flame at 1024 psig. Note the increase in intensity of the core flame structure from Figure 12 at 418 psig.**

That the flame of combusting nitromethane appears to intensify throughout the increase in pressure corresponds with a logarithmic increase in pressurization as a result of gasifying propellant. This reliability of pressure rise further indicates the viability of nitromethane in rocket engine applications in which targetable, consistent pressure is required for dependable performance at steady-state conditions. Figure 14 demonstrates the mass-corrected pressure rise in psig/g versus burning rate in mm/s.

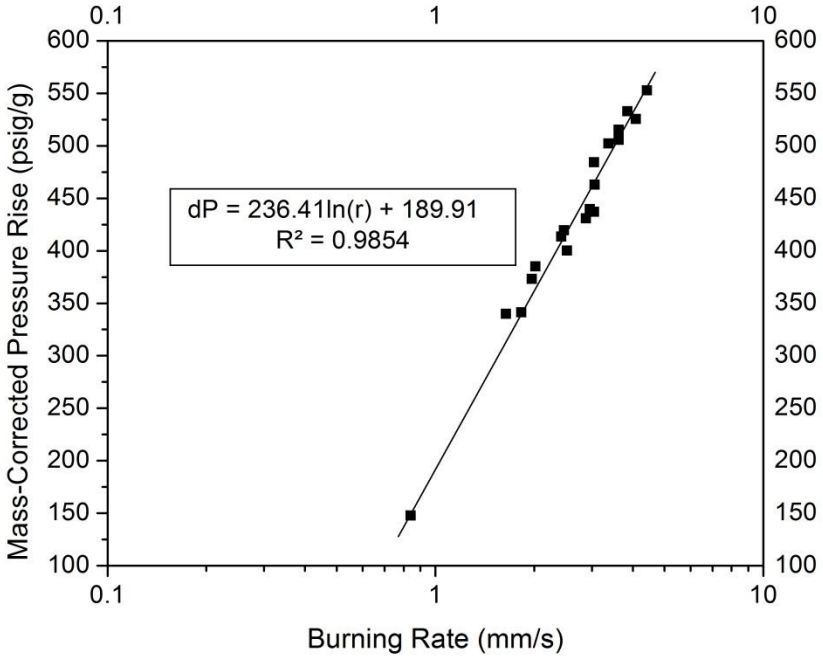


**Figure 14. Logarithmic curve-fit of pressurization of propellant versus burning rate**

Though a viable and proven monopropellant, nitromethane presents difficulties to ignition under inert environments as discovered during initial experiments as well as

noted by Boyer (2005) and Birk et al. (1992). Ignition using the current-heated wire method could not be achieved in the present study under an inert, argon atmosphere at pressures up to 4000 psig. However, under a pressurized environment of 79% argon and 21% oxygen, ignition could be achieved reliably. The presence of oxygen in the pressurant gas acts merely as a booster for initial ignition; once the propellant is burning in the cavity, it is deducted that the nitromethane burns solely as a monopropellant, as the main reaction zone occurs below the surface of the cavity in the absence of outside oxidizer. All other recent studies have been forced to employ some sort of ignition booster for initial nitromethane ignition and start-up transient, including an oxygen/hydrocarbon non-premixed flame (Yetter et al, 2007), compressed air pressurant (Boyer, 2005; Kelzenberg et al, 1999), or a solid propellant booster under an inert atmosphere (Boyer 2005).

However, at pressures below 350-400 psig, ignition using the normal methods proved markedly more difficult. This behavior is a very similar phenomenon as was encountered by the Penn State-Princeton group working on a nitromethane microthruster (Yetter et al., 2007). Often, strands in the present study would not ignite before the nichrome wire reached its melting temperature, forcing the cessation of the experiment. When ignition did occur, analysis revealed an abnormal pressure profile for these low-pressure burns. Inspection of the light emission trace revealed a throbbing or oscillating behavior as shown in Figure 15. It is conjectured that this pulsing is a result of heated nitromethane vapor combusting with the oxygen pressurant without preheating the propellant strand to a sufficient temperature to sustain monopropellant combustion.

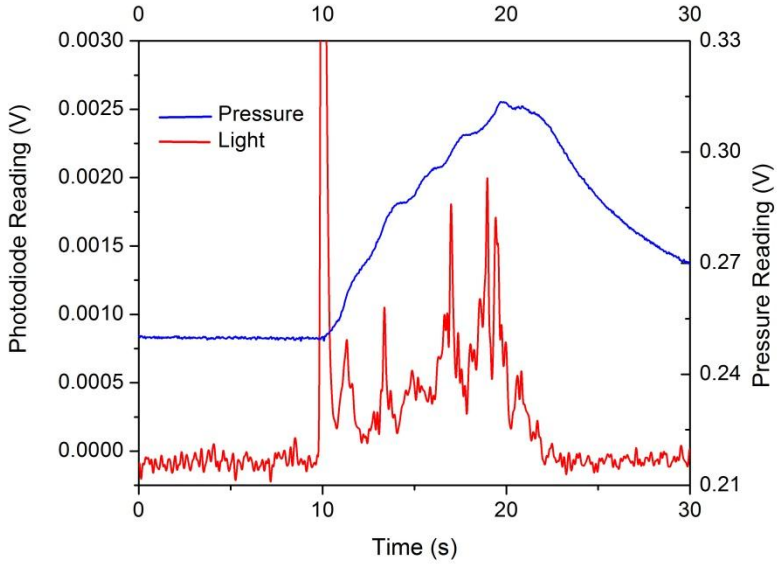


**Figure 15. Abnormal profiles for a run under 350 psig. Note the instances of oscillating pressure rise coincident with spikes in light emission.**

## 4.2 Burning Rate

As described in more detail in section 3.4.3, calculation of the burning rate of a propellant is derived from the total burning time, known dimensions of the propellant cavity, and known density of the propellant. For the pressure regime in this study according to Equation 19, the burning rate was calculated from the data as

$$r = 0.002*P^{1.02} \tag{30}$$

where $r$ is in mm/s and $P$ is in psig (for P in units of MPa, $a = 0.3537$).

Table 2 displays the useful information from the series of burns of nitromethane in the strand burner with pressures ranging from 418 to 1910 psig.

**Table 2. Burning Rate data for pressures from 418-1910 psig (2.88-13.17MPa)**

| Bomb Pressure | | $m_p$ | t | $\dot{m}$ | r | r |
|---|---|---|---|---|---|---|
| psig | MPa | grams | sec | g/s | mm/s | in/s |
| 1910 | 13.17 | 0.60 | 1.823 | 0.33 | 4.50 | 0.18 |
| 1867 | 12.87 | 0.63 | 1.949 | 0.32 | 4.42 | 0.17 |
| 1800 | 12.41 | 0.62 | 2.072 | 0.30 | 4.09 | 0.16 |
| 1643 | 11.33 | 0.63 | 2.237 | 0.28 | 3.85 | 0.15 |
| 1594 | 10.99 | 0.63 | 2.376 | 0.27 | 3.62 | 0.14 |
| 1534 | 10.58 | 0.63 | 2.378 | 0.26 | 3.62 | 0.14 |
| 1441 | 9.93 | 0.64 | 2.593 | 0.25 | 3.37 | 0.13 |
| 1348 | 9.30 | 0.63 | 2.820 | 0.22 | 3.05 | 0.12 |
| 1243 | 8.57 | 0.64 | 2.854 | 0.22 | 3.06 | 0.12 |
| 1218 | 8.40 | 0.64 | 2.955 | 0.22 | 2.96 | 0.12 |
| 1185 | 8.17 | 0.63 | 2.825 | 0.22 | 3.05 | 0.12 |
| 1143 | 7.88 | 0.63 | 2.985 | 0.21 | 2.88 | 0.11 |
| 1098 | 7.57 | 0.63 | 3.479 | 0.18 | 2.47 | 0.10 |
| 1024 | 7.06 | 0.63 | 3.560 | 0.18 | 2.42 | 0.10 |
| 971 | 6.69 | 0.64 | 3.475 | 0.18 | 2.52 | 0.10 |
| 929 | 6.40 | 0.64 | 3.838 | 0.17 | 2.28 | 0.09 |
| 855 | 5.90 | 0.63 | 4.257 | 0.15 | 2.02 | 0.08 |
| 806 | 5.56 | 0.64 | 4.428 | 0.14 | 1.97 | 0.08 |
| 747 | 5.15 | 0.63 | 4.714 | 0.13 | 1.83 | 0.07 |
| 665 | 4.59 | 0.63 | 5.236 | 0.12 | 1.64 | 0.06 |
| 418 | 2.88 | 0.63 | 10.307 | 0.06 | 0.84 | 0.03 |

Subsequently, Figure 16 shows these burning rates plotted as a function of pressure, with appropriate error bars reflecting the uncertainty calculated as described in section 3.4.3.

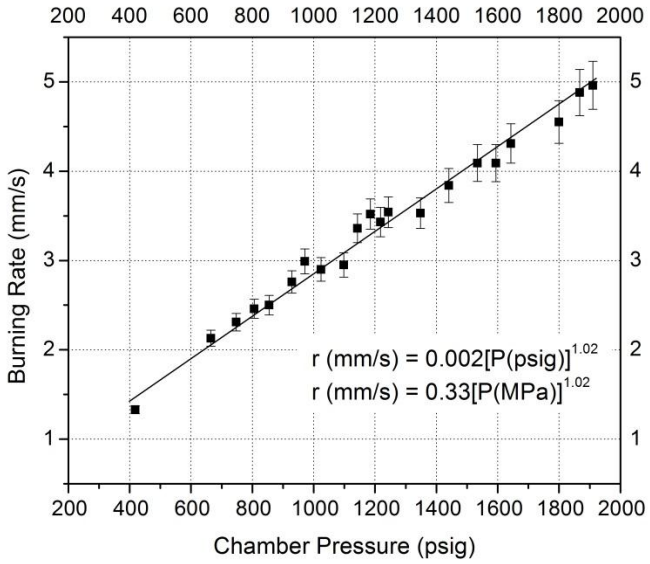


**Figure 16. Data from current study with burning rate power correlation**

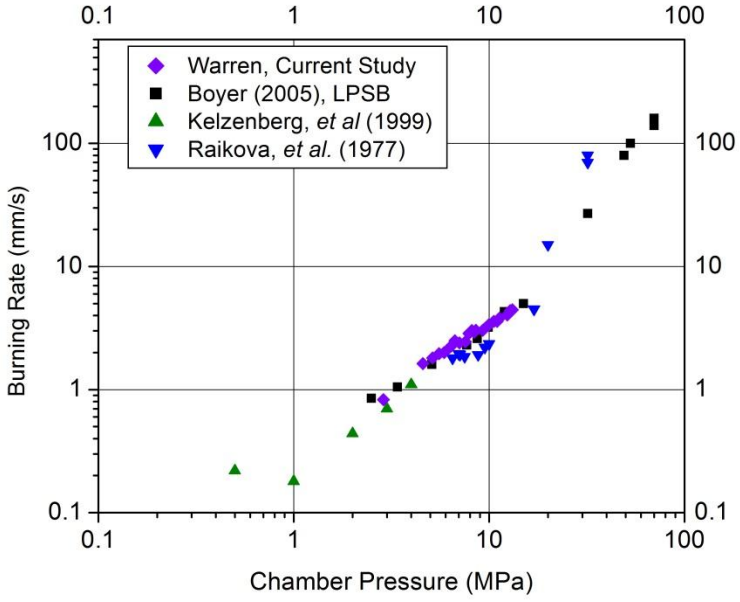


**Figure 17. Overlay of current study data with that from literature in similar pressure regions.**

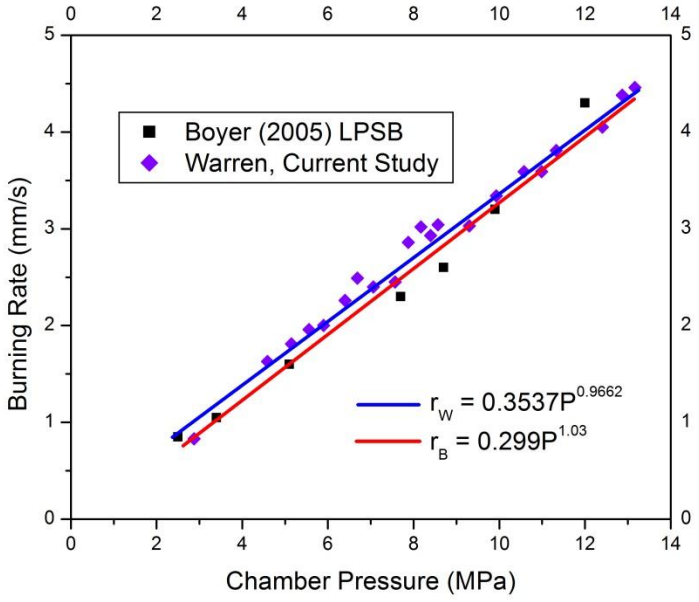


**Figure 18. Comparison of data from current study with most recent burning rate correlation of methane in literature, Boyer (2005). Note the burning rate in this chart is a function of pressure in MPa, rather than psig as correlated above.**

As can be seen in Figures 17 and 18, which shows the present results with results from previous studies, the burning rate of nitromethane under the current experimental setup is generally less than 0.1 mm/s higher than that of other published rates in the same pressure regimes. This slight increase can be accounted for by the fact that the propellant in the current study is uniformly heated upon ignition as a result of heating element configuration, whereas in studies from Boyer (2005), Kelzenberg et al. (1999), Rice and Cole (1953), and Raikova (1977), a flame either progresses into a cooler, quiescent strand or is uniformly fed propellant via pumping system. In each of the cases, the

temperature dependence of the pre-exponential factor *a* from Equation 19 becomes evident, accelerating the burning rate across the spectrum of pressures utilized but retaining a very similar pressure exponent *n*.

It should be noted that there exists a region of data for burns below 350 psig that, using a slightly altered measurement of burning time, appears to have a larger *n* value leading to a steepened burning rate curve. However, confirmation of these initial results are not currently available as the normal method of measuring burning time does not properly account for the pulsing burning behavior at the low pressure regime. The multi-spike pattern as seen in Figure 15 causes an increase in measured burning time as well as dramatically reducing reliability when using the main method described in Section 3.4.2. Future experiments may be used to focus on this region of burning.

# 5. SUMMARY AND CONCLUSIONS

## 5.1 Experimental Objectives Achieved

- Developed techniques for igniting small samples of liquid propellant within a strand bomb apparatus at high pressure.
- Burning rate measurements were taken for nitromethane at pressures ranging from 418 to 1910 psig, resulting in a burning rate curve of

$$r\ (mm/s) = 0.33[P(MPa)]^{1.02} \tag{31}$$

$$r\ (mm/s) = 0.0021[P(psig)]^{1.02} \tag{32}$$

- Plans were established for future experimental methods to investigate advanced HAN-based monopropellants in both strand burner and shock-tube configuration.

## 5.2 Recommendations for Future Work

### 5.2.1 Changes to Equipment

Observing the combustion behavior of nitromethane under various conditions, it is recommended that certain design changes be made to a future strand bomb apparatus to improve burning of the propellant as well as data acquisition. The first of these design changes would be the shifting of the location of the three lateral optical ports to better observe the location of the propellant. Because the ports are designed, and currently

aligned, to capture the ignition of an elevated strand of solid propellant, the ability to visually observe strand ignition of liquid propellants is less than ideal.

Secondly, minor uncertainty in linear burning rate could be mitigated by reducing the potential for abnormal burning surface geometry as a result of surface turbulence during the burn. This reduction could be achieved by machining a new burner plug with an enlarged propellant cavity diameter. The enlarged cavity would lessen the chance of localized surface abnormalities - that are a result of rapid boiling beneath the liquid propellant surface for HAN-based propellants as shown in Figure 10 - from affecting the global average surface geometry. Unfortunately, stocks from available suppliers of fully threaded steel bolts in the correct diameter and depth are limited generally to 1 inch in diameter and 3 inches in threaded length. Were the burner plug to be revamped, the case would arise in which either a custom bolt would need to be ordered at increased price, or another partially threaded bolt would need to be machined to specification. In this case, a custom-designed bolt would be preferable, as tolerances would be assumed more reliable and multiple bolts could be ordered from a single supplier with minimal aberrations in dimension.

Finally, and most radically differing from the current apparatus, a propellant feed system could be installed, which would allow for longer burning times. An increase in experiment time would allow combustion to reach a somewhat steady state within the bomb, providing better conditions for visual inspection of the burning event. This feed system could be achieved with a transparent quartz tube inserted through the underside of the bomb, through which a given propellant could be fed upwards via piston. The feed

rate would be established from prior static experiments, and could be altered prior to the experiment or possibly during.

Further results at high pressures would give a more-complete view of nitromethane burning behavior. The central obstacle in studying the combustion behavior of nitromethane is overcoming problems with its ignitability; once at steady combustion, nitromethane burns self-sustainingly until all the propellant is exhausted. Boyer (2005) utilized an ammonium perchlorate-based solid propellant as a booster in an UHPSB setup to achieve ignition in an inert atmosphere. The Propellant Laboratory has a store of AP-based propellants and the expertise to mix and cure these reliably. However, using the current method of calculating burning time, it would be prohibitively difficult to discern the burn time of liquid propellant from that of the solid propellant from the pressure and light data acquired. A larger strand with better optical access that would allow for longer burn times could be used in future experiments at these elevated pressures.

Were the three of these possible improvements to the experimental apparatus to be implemented, the effort would require a near-complete revamping of the facility. The cost of materials, planning, and time would be high, but the results of the redesign could open doors to novel methods for investigating the combustion behavior of a wide range of liquid fuels, both rocket propellants and other chemicals. The case can also be made to install a separate liquid propellant apparatus in the test cell immediately adjacent to the current test cell, which would still have easy access to the control room as well as all current DAQ and safety equipment. Further, an automated control and data acquisition

system, such as LabView from National Instruments, should be implemented to further improve repeatability among experiments.

### 5.2.2 Changes to Propellant

Because of the interest in improved safety and stability of advanced monopropellants, there exists interest in the pairing of nitromethane with an aqueous, HAN propellant base. Currently there is little literature pertaining to such a mixture, but the nature of the two fuels points promisingly to a potential as a viable candidate for a blended monopropellant mixture. Hydroxylammonium nitrate, as available to civilian customers, is sold exclusively in highly dilute, aqueous solutions; dilute to the point of negligible energetic potential in the current experimental setup. However, because of the extremely low vapor pressure of pure HAN, it is predicted that the water content of such a solution could be reduced through vacuum desiccation to yield HAN in appropriate proportion. Once refined through the desiccation process, the HAN/$H_2O$ solution would be blended with nitromethane to produce a new, potential monopropellant.

### 5.2.3 Other Experiments in Progress

Presently in progress in the Propellant Laboratory is the development of methods for studying the ignition of liquid rocket monopropellants in a shock-tube apparatus. An aerosol injection technique will be utilized to suspend ultra-fine micron-scale particles of

low vapor pressure propellants such as HAN-based EILs. A shock-tube proves extremely useful as a result of its ability to use the Rankine-Hugoniot shock relations to establish targetable, repeatable test conditions. These shock-tube experiments would be vital for verifying and improving a chemical kinetics mechanism for any of the studied propellants.

# REFERENCES

Aerojet-General Corp. 1958. “Some Considerations Pertaining to Space Navigation.” Special Report No. 1450, 18.

Alfano, A., Mills, J., and Vaghjiani, G. 2009 "Resonant Laser Ignition Study of HAN-HEHN Propellant Mixture." *Combustion Science and Technology.* **181**, 6.

Birk, A., McQuaid, M., and Bliesener, G., 1992, *Reacting Liquid Monopropellant Sprays -Experiments with High Velocity Full Cone Sprays in 33 MPa, 500 °C Nitrogen*, ARL, Report ARL-TR-17.

Boyer, E. 2005 “Combustion Characteristics and Flame Structure of Nitromethane Liquid Monopropellant.” Ph.D. Dissertation. The Pennsylvania State University.

Boyer, E., and Kuo, K. K. 1999. “High-pressure combustion behavior of nitromethane” *35th AIAA/ASME/SAE/ASEE Joint Propulsion Conference and Exhibit*, Los Angeles, CA, June 20-24, 1999.

Carro, R.V. 2001. “High Pressure Testing of Composite Solid Rocket Propellant Mixtures: Burner Facility Characterization.” Master’s Thesis. University of Central Florida.

Chang, Y.P., Kuo, K.K.. Boyer, E. 2000. “Intrinsic Burning Behavior and Flame Structure Diagnostics of Liquid Propellants.” U.S. Army Research Office. Report No. 20001124 014.

*CRC Handbook of Chemistry and Physics*. 44th ed. CRC, 1962.

Czysz, Paul A., and Bruno, C. 2006. *Future Spacecraft Propulsion Systems: Enabling Technologies for Space Exploration*. Springer, Berlin.

Dow Chemical Company. 2011. “Nitromethane.” Angus Technical Bulletin. CAS Reg. No. 75-52-5

Edwards, T. 2003. "Liquid Fuels and Propellants for Aerospace Propulsion: 1903-2003." *Journal of Propulsion and Power*. **19,** 6.

Fokema, M. D., and Torkelson, J. E., 2007. “Thermally Stable Catalyst and Process for the Decomposition of Liquid Propellants.” Aspen Products Group, assignee. Patent 11/457,985.

Fortini, A. J., Babcock, J. R., and Wright, M. J. 2008. “Self-Adjusting Catalyst for Propellant Decomposition.” Patent 11/283,575.

Hawkins, T. W., Brand, A. J., McKay, M. B. and Tinnirello, M. 2010. "Reduced Toxicity, High Performance Monopropellant at the U.S. Air Force Research Laboratory." *Proc. of 4th International Association for the Advancement of Space Safety Conference*, Huntsville, AL.

Interstate Commerce Commission. Tuggle, Commissioner. 1958. “Accident Near Mt. Pulaski, ILL.” Ex Parte No 213.

Jankovsky, R. S., 1996. "HAN-Based Monopropellant Assessment for Spacecraft." *Proc. of 32nd Joint Propulsion Conference*, Lake Buena Vista, Florida.

Jones, P., Hawkins, T., Brand, A., McKay, M., Ismail, I., and Warmouth. G. 2002. "Characterization of 2-Hydroxyethylhydrazine (HEH) and 2-Hydroxyethylhydrazinium Nitrate (HEHN)." *Proc. of JANNAF Propellant*

*Development and Characterization Subcommittee Conference*, Colorado Springs, CO.

Kelzenberg, S., Eisenreich, N., Eckl, W., and Weiser, V. 1999. "Modelling Nitromethane Combustion." *Propellants, Explosives, Pyrotechnics*. **24,** 3.

Kreitz, K. 2010. "Catalytic Nanoparticle Additives in the Combustion of AP/HTPB Composite Solid Propellant." Master's Thesis. Texas A&M University.

Moffat, R.J. 1982. Contributions to the Theory of Single-Sample Uncertainty Analysis. Journal of Fluids Engineering. **104**.

Mueller, J. 1997. "Thruster Options for Microspacecraft: A Review and Evaluation of Existing Hardware and Emerging Technologies" AIAA 97-3058.

National Aeronautics and Space Administration (NASA). 1988. "Space Shuttle News Reference Manual."

Office of Environmental Health Hazard Assessment (OEHHA), California Environmental Protection Agency. 2000. "Chronic Toxicity Summary." Determination of Noncancer Chronic Reference Exposure Levels. Batch 2A.

Raikova, V. M. 1977 "Limit Conditions of Combustion and Detonation of Nitroesters and Mixtures on their Base." Ph.D. Thesis. Mendeleev Institute of Chemical Technology, Moscow.

Rice, T. K. and Cole, Jr., J. B., 1953. *Liquid Monopropellants Burning Rate of Nitromethane*, Naval Ordnance Lab Report NAVORD-2885, White Oak, MD.

Sabourin, J. L., Dabbs, D.M., Yetter, R.A., Dryer, F.L., and Aksay, I.A. 2009. "Functionalized Graphene Sheet Colloids for Enhanced Fuel/Propellant Combustion." *ACS Nano*. **3,** 12.

Smiglak, M., Reichert, W. M., Holbrey, J. D., Wilkes, J. S., Sun, L., Thrasher, J. S., Kirichenko, K., Singh, S., Katritzky, A. R. and Rogers, R. D. 2006. "Combustible Ionic Liquids by Design: Is Laboratory Safety Another Ionic Liquid Myth?" *Chemical Communications.* **24.**

Sutton, G. P., and Biblarz, O. 2001. *Rocket Propulsion Elements*. New York: John Wiley & Sons.

Vosen, S. 1990. "Hydroxylammonium Nitrate-based Liquid Propellant Combustion-interpretation of Strand Burner Data and the Laminar Burning Velocity." *Combustion and Flame.* **82,** 3-4.

Ward, T.A., 2010 *Aerospace Propulsion Systems*. John Wiley & Sons, Singapore.

Yetter, R.A. and Rabitz, H. 1989. "Modeling and Sensitivity Analysis of Homogeneous Gas-Phase Nitromethane Decomposition." Technical Report 1854. Department of Mechanical and Aerospace Engineering. Princeton University, Princeton, NJ.

Yetter, R.A., Yang, V., Wu M., Wang, Y., Milius, D., Aksay, I.A., and Dryer, F.L, 2007. "Combustion Issues and Approaches for Chemical Microthrusters." *International Journal of Energetic Materials and Chemical Propulsion.* **6**, 4.

# APPENDIX A

## SAFETY INFORMATION

The following are safety steps taken by the Propellant Laboratory to ensure the safety of research personnel and technicians:

- Personnel wear safety equipment appropriate for the propellant being handled. For most hydrocarbons, neoprene or nitrile gloves and full-face respirators are employed. However, for more toxic substances, full body chemical splash suits are available.
- Rubber-soled shoes are worn at all times to reduced buildup of static charges.
- Emergency eye-wash and shower are available in the testing area in case of emergency caused by contamination.
- Propellant is contained in secure explosives magazines; or if not independently explosives, in flame-resistant cabinets
- The floor in the laboratory is a multi-feet deep floating concrete slab coated with an electro-static dissipating (ESD) epoxy, drastically reducing the danger of accidental ignition of a propellant by errant static charges.
- Reinforced concrete blast walls and steel blast doors isolate the test cell whenever the strand bomb is pressurized.
- Ventilation for the propellant lab is fed into the main exhaust system for the building and when activated evacuates and recycles the air in the lab within 90 seconds.

- In case of emergency, fire suppression equipment includes a sodium chloride powder extinguisher for metal fires and those involving strong solid propellant oxidizers, two carbon-dioxide extinguishers for most other flames, and finally building-wide sprinkler system.


**Figure A1. Safety Equipment. Explosives magazine and example of safety equipment that can be worn by personnel depending on the toxicity and/or carcinogenicity of a given rocket propellant. Included above are full-face respirator, Tychem SL chemical splash suits, neoprene gloves, and low static, rubber-soled footwear.**

# APPENDIX B

# EXPERIMENTAL PROCEDURE

## Preparing the laboratory for testing

1. Data Acquisition (DAQ) computers and software are booted up and appropriate settings applied within DAQ software
2. Materials need for experiment are retried from storage: nickel-chromium wire, wire cutters, Kim-wipes, cotton swabs, acetone,
3. Dummy bolt is removed from strand bomb and set aside, leaving the burner bolt orifice open on the underside of the strand bomb.
4. Negative lead from power supply is attached to the negative lead from the bomb, on one side of the electrical relay.

## Preparing the burner bolt

5. Entire burner bolt surface is scoured and cleaned with acetone to prevent contamination of propellant from possible residue.
6. At start of each round of experiments, fresh PTFE thread tape is applied to the threads of the burner bolt if previous tape appears to have any significant wear.
7. Electrical leads are scoured to expose bare metal, ensuring a clean connection for nichrome wire.
8. Nichrome wire is cut to length of approximately 4.5-5 inches.

9. One end of wire is wrapped around the top edge of the negative lead, drooped as far as possible into the propellant cavity, and out again to be wrapped and secured to the top edge of the copper positive lead.
10. Wire is manipulated to ensure no contact with the bolt itself, in order to provide uniform and repeatable current flow and heating.
11. Small amount of propellant is removed from its storage vessel via a plastic dropper. The dropper is then placed up-ended in a beaker on the scale, which is then tared to a reading of 0.00 grams.
12. Enough propellant to fill the cavity to be flush with the top surface of the bolt is deposited in the cavity.

*The bolt is now prepared for insertion into the testing apparatus.*

13. SAFETY SWITCH is flipped to the ON position, activating the control panel.
14. ARGON FILL switch is engaged, which opens the solenoid fill valve, flushing the bomb with a burst of high pressure argon, which dissipates from the open bolt orifice, and subsequently the argon gas within the bomb quickly reaches a steady-state pressure of 3-4 psig.
15. Readied burner bolt is inserted into the orifice on the underside of the strand bomb, and is screwed into the threads in the orifice and tightened into place with a wrench, sealing the bomb.
16. Positive lead on bolt attached to positive lead from power supply.
17. Power supply is turned on.

18. Blast door is closed and secured.
19. Lights are extinguished in the laboratory and personnel return to control room.

**Burning Sample**

*Once the sample has been inserted into the strand bomb and all electrical connections are established, the test can begin.*

20. Pressure is allowed to rise until roughly 5% above desired test pressure. ARGON FILL switch is then turned to the off position. Pressure will then fall as transient gas effects within the apparatus equalize.
21. Once pressure has equalized, GageScope DAQ software is triggered.
22. Upon confirmation software has successfully triggered, IGNITION button is pressed and held for duration of experimental run.
23. At completion of the test time, the exhaust vent to the bomb is opened via the EXHAUST switch.
24. As the bomb depressurizes, data from the experiment is saved in two copies, a *.sig file for future GageScope examination, and *.asc file extension for use in spreadsheet programs and for analysis in Origin or MATLAB.

**Resetting equipment**

25. Upon complete depressurization of the bomb back to atmospheric pressure, the power supply is turned off, the electrical connections detached, and the burner bolt is removed and taken to the fume hood.

26. Any residue left in the burner cavity is assumed to be unburnt propellant. This residual propellant is then swabbed and weighed. The difference between pre-burnt propellant mass and post-burn propellant mass is considered the mass consumed by combustion during the experiment.
27. The bolt is then completely cleaned again, returning the process back to step 6 to be repeated as long as experiments take place.

*Once experiments are completed for a particular session of burns:*

28. The burner bolt is swabbed and cleaned, with the exposed surfaces of the bolt covered in a thin layer of vacuum grease to prevent oxidation of the bolt surface.
29. The dummy bolt is reinserted into the strand bomb, and the bomb is pressurized to about 200 psig of argon, then rapidly depressurized. This ensured a satisfactory purge of non-inert gasses and helps prevent unwanted oxidation along the walls of the bomb. Once the pressure returns to atmosphere, the SAFETY SWITCH is flipped to the OFF position and the control panel is considered safe.
30. Materials are returned to their storage locations.

# APPENDIX C

## BURNER BOLT CAD MODEL

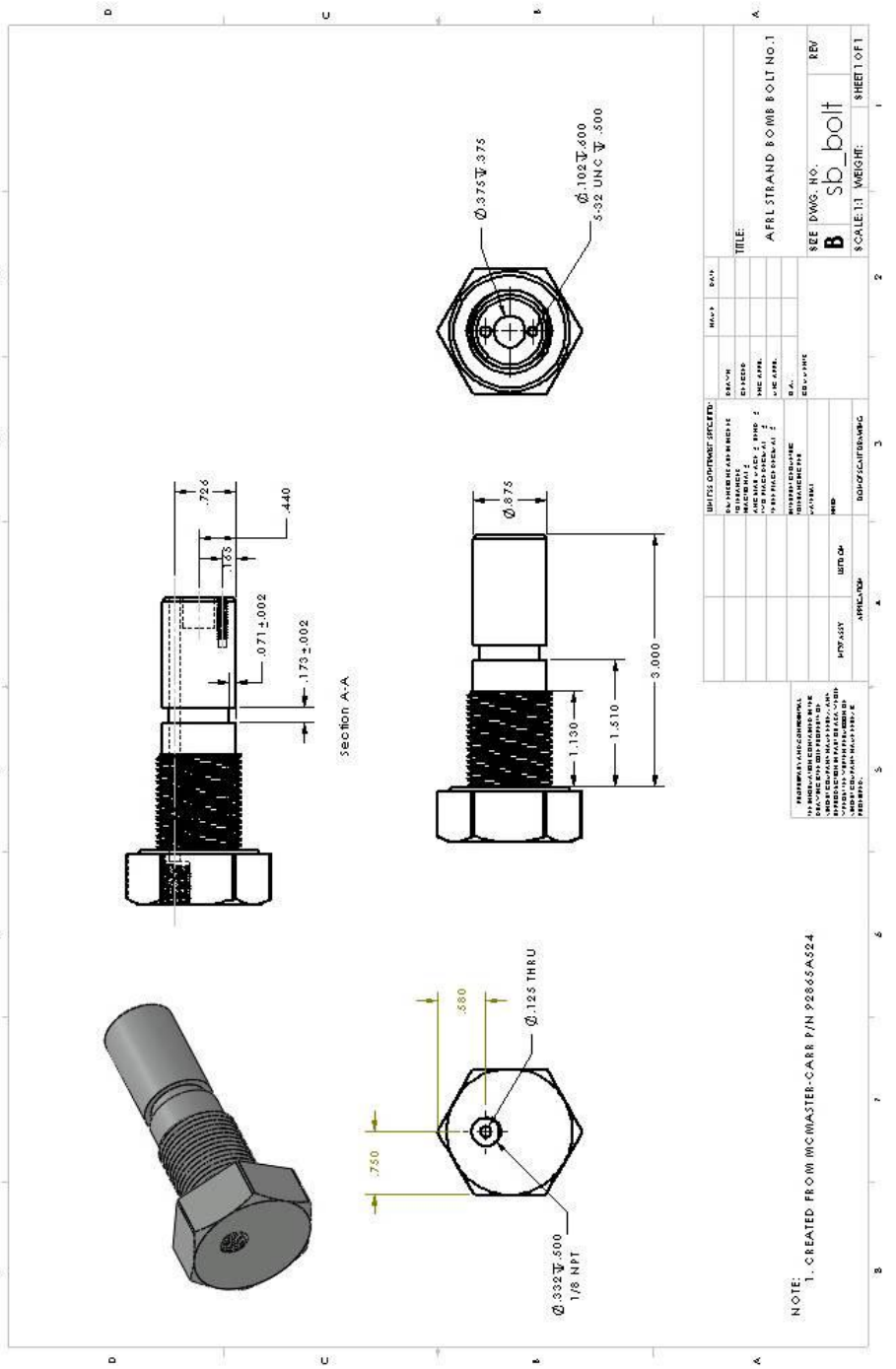


**Figure 20. Burner bolt CAD model**

APPENDIX D

GAGESCOPE SCREENSHOT

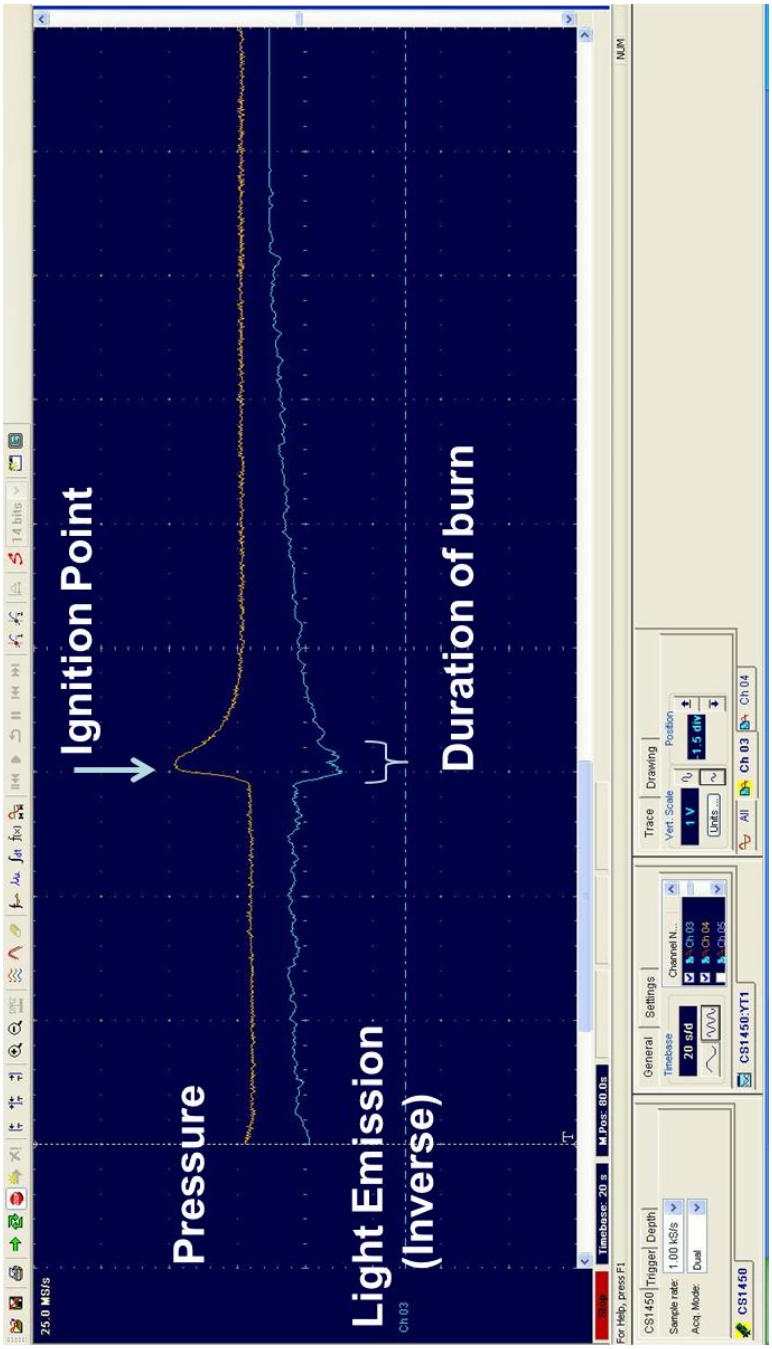


**Figure 21. Screenshot of Gagescope data acquisition software for experimental run.**

# APPENDIX E

**Table E1. Manufacturer information and model numbers for transducers, filters, cameras, spectrometer, and other equipment**

| | Type | Maker | Model | Quantity |
|---|---|---|---|---|
| Hardware | | | | |
| | Pressure Transducer | OmegaDyne | PX02C1-7.5KG5T | 2 |
| | Photodiode | New Focus | 2031 | 1 |
| | Spectrometer | OceanOptics | USB2000 | 1 |
| | Detector | Sony | ILX511A | 1 |
| | High Pressure Feed-through Gland | Conax | PL-14-1 | 1 |
| | Electric Relay | Struthers-Dunn | 0339AF | 1 |
| | Bolt | McMaster-Carr | 92620A957 | 1 |
| | Power Supply | GW Instek | SPS-3610 | 1 |
| | Scale | Ohaus | ARA520 | 1 |
| | Fume Hood | Labconco | 608040010814 | 1 |
| | Nickel Chromium wire | Consolidated | AWG 30 | 1 |
| | Full-Face Respirator | Sperian | 7620 | 2 |
| | Filters (P100 Org Vap) | Sperian | 1053 NIOSH | 4 |
| Software | | | | |
| | Oscilloscope | GageScope | | 1 |
| | Data processing | Microsoft | Excel 2010 | 1 |
| | Graphic visualization | Origin | Origin 8.1 and 6.1 | 1 |
| | Modeling | Math Works | MATLAB 2010a | 1 |

# APPENDIX F

## CEA Output for Nitromethane as Monopropellant

```
******************************************************************************

        NASA-GLENN CHEMICAL EQUILIBRIUM PROGRAM CEA2, MAY 21, 2004
                  BY  BONNIE MCBRIDE AND SANFORD GORDON
      REFS: NASA RP-1311, PART I, 1994 AND NASA RP-1311, PART II, 1996

******************************************************************************
problem   case=test2
    rocket  equilibrium  frozen  nfz=1  tcest,k=3000
  p,psia=1000,
  sub,ae/at=50,
  sup,ae/at=50,
react
  name=CH3NO2(L) wt=100  t,k=298
end

OPTIONS: TP=F  HP=F  SP=F  TV=F  UV=F  SV=F  DETN=F  SHOCK=F  REFL=F  INCD=F
RKT=T  FROZ=T  EQL=T  IONS=F  SIUNIT=T  DEBUGF=F  SHKDBG=F  DETDBG=F  TRNSPT=F

TRACE= 0.00E+00  S/R= 0.000000E+00  H/R= 0.000000E+00  U/R= 0.000000E+00

Pc,BAR =    68.947304

Pc/P =

SUBSONIC AREA RATIOS =    50.0000

SUPERSONIC AREA RATIOS =    50.0000

NFZ=  1  Mdot/Ac= 0.000000E+00  Ac/At= 0.000000E+00

   REACTANT          WT.FRAC   (ENERGY/R),K   TEMP,K  DENSITY
       EXPLODED FORMULA
N: CH3NO2(L)        1.000000  -0.136027E+05   298.00  0.0000
         C  1.00000  H  3.00000  N  1.00000  O  2.00000

 SPECIES BEING CONSIDERED IN THIS SYSTEM
(CONDENSED PHASE MAY HAVE NAME LISTED SEVERAL TIMES)
 LAST thermo.inp UPDATE:    9/09/04

 g 7/97  *C               tpis79  *CH              g 4/02  CH2
 g 4/02  CH3              g11/00  CH2OH            g 7/00  CH3O
 g 8/99  CH4              g 7/00  CH3OH           srd 01  CH3OOH
 g 8/99  *CN              g12/99  CNN             tpis79  *CO
 g 9/99  *CO2             tpis91  COOH            tpis91  *C2
 g 6/01  C2H              g 1/91  C2H2,acetylene  g 5/01  C2H2,vinylidene
 g 4/02  CH2CO,ketene     g 3/02  O(CH)2O          srd 01  HO(CO)2OH
 g 7/01  C2H3,vinyl       g 9/00  CH3CN            g 6/96  CH3CO,acetyl
 g 1/00  C2H4             g 8/88  C2H4O,ethylen-o  g 8/88  CH3CHO,ethanal
 g 6/00  CH3COOH          srd 01  OHCH2COOH        g 7/00  C2H5
 g 7/00  C2H6             g 8/88  CH3N2CH3         g 8/88  C2H5OH
 g 7/00  CH3OCH3          srd 01  CH3O2CH3         g 7/00  CCN
 tpis91  CNC              srd 01  OCCN             tpis79  C2N2
 g 8/00  C2O              tpis79  *C3              n 4/98  C3H3,1-propynl
 n 4/98  C3H3,2-propynl   g 2/00  C3H4,allene      g 1/00  C3H4,propyne
 g 5/90  C3H4,cyclo-      g 3/01  C3H5,allyl       g 2/00  C3H6,propylene
 g 1/00  C3H6,cyclo-      g 6/01  C3H6O,propylox   g 6/97  C3H6O,acetone
```

```
 g 1/02  C3H6O,propanal   g 7/01  C3H7,n-propyl    g 9/85  C3H7,i-propyl
 g 2/00  C3H8             g 2/00  C3H8O,1propanol  g 2/00  C3H8O,2propanol
 srd 01  CNCOCN           g 7/88  C3O2             g tpis  *C4
 g 7/01  C4H2,butadiyne   g 8/00  C4H4,1,3-cyclo-  n10/92  C4H6,butadiene
 n10/93  C4H6,1butyne     n10/93  C4H6,2butyne     g 8/00  C4H6,cyclo-
 n 4/88  C4H8,1-butene    n 4/88  C4H8,cis2-buten  n 4/88  C4H8,tr2-butene
 n 4/88  C4H8,isobutene   g 8/00  C4H8,cyclo-      g10/00  (CH3COOH)2
 n10/84  C4H9,n-butyl     n10/84  C4H9,i-butyl     g 1/93  C4H9,s-butyl
 g 1/93  C4H9,t-butyl     g12/00  C4H10,n-butane   g 8/00  C4H10,isobutane
 g 6/01  C4N2             g 8/00  *C5             g 5/90  C5H6,1,3cyclo-
 g 1/93  C5H8,cyclo-      n 4/87  C5H10,1-pentene  g 2/01  C5H10,cyclo-
 n10/84  C5H11,pentyl     g 1/93  C5H11,t-pentyl   n10/85  C5H12,n-pentane
 n10/85  C5H12,i-pentane  n10/85  CH3C(CH3)2CH3    g 2/93  C6H2
 g11/00  C6H5,phenyl      g 8/00  C6H5O,phenoxy    g 8/00  C6H6
 g 8/00  C6H5OH,phenol    g 1/93  C6H10,cyclo-     n 4/87  C6H12,1-hexene
 g 6/90  C6H12,cyclo-     n10/83  C6H13,n-hexyl    g 6/01  C6H14,n-hexane
 g 7/01  C7H7,benzyl      g 1/93  C7H8             g12/00  C7H8O,cresol-mx
 n 4/87  C7H14,1-heptene  n10/83  C7H15,n-heptyl   n10/85  C7H16,n-heptane
 n10/85  C7H16,2-methylh  n 4/89  C8H8,styrene     n10/86  C8H10,ethylbenz
 n 4/87  C8H16,1-octene   n10/83  C8H17,n-octyl    n 4/85  C8H18,n-octane
 n 4/85  C8H18,isooctane  n10/83  C9H19,n-nonyl    g 3/01  C10H8,naphthale
 n10/83  C10H21,n-decyl   g 8/00  C12H9,o-bipheny  g 8/00  C12H10,biphenyl
 g 6/97  *H               g 6/01  HCN              g 1/01  HCO
 tpis89  HCCN             g 6/01  HCCO             g 6/01  HNC
 g 7/00  HNCO             g10/01  HNO              tpis89  HNO2
 g 5/99  HNO3             g 4/02  HO2              tpis78  *H2
 g 5/01  HCHO,formaldehy  g 6/01  HCOOH            g 8/89  H2O
 g 6/99  H2O2             g 6/01  (HCOOH)2         g 5/97  *N
 g 6/01  NCO              g 4/99  *NH              g 3/01  NH2
 tpis89  NH3              tpis89  NH2OH            tpis89  *NO
 g 4/99  NO2              j12/64  NO3              tpis78  *N2
 g 6/01  NCN              g 5/99  N2H2             tpis89  NH2NO2
 g 4/99  N2H4             g 4/99  N2O              g 4/99  N2O3
 tpis89  N2O4             g 4/99  N2O5             tpis89  N3
 g 4/99  N3H              g 5/97  *O              g 4/02  *OH
 tpis89  *O2              g 8/01  O3              n 4/83  C(gr)
 n 4/83  C(gr)            n 4/83  C(gr)           g11/99  H2O(cr)
 g 8/01  H2O(L)           g 8/01  H2O(L)

O/F =   0.000000

                        EFFECTIVE FUEL     EFFECTIVE OXIDANT        MIXTURE
ENTHALPY                    h(2)/R             h(1)/R               h0/R
(KG-MOL)(K)/KG       -0.22284930E+03     0.00000000E+00     -0.22284930E+03

KG-FORM.WT./KG             bi(2)              bi(1)              b0i
 *C                   0.16382695E-01     0.00000000E+00     0.16382695E-01
 *H                   0.49148084E-01     0.00000000E+00     0.49148084E-01
 *N                   0.16382695E-01     0.00000000E+00     0.16382695E-01
 *O                   0.32765389E-01     0.00000000E+00     0.32765389E-01

POINT ITN      T            C           H           N           O

  1   18    2461.032     -11.021      -8.714     -12.610     -19.864

Pinf/Pt = 1.790534
  2    3    2203.909     -10.589      -8.810     -12.708     -21.134

Pinf/Pt = 1.795521
  2    2    2202.732     -10.587      -8.810     -12.708     -21.141

  3    1    2461.024     -11.021      -8.714     -12.610     -19.864
```

```
  3    1    2461.012     -11.021      -8.714     -12.610     -19.864

  4   11     771.103      -1.193     -10.236     -14.236     -45.787

ADD  C(gr)
  4    1     771.136      -1.194     -10.236     -14.236     -45.785

  4    3     782.116      -1.210     -10.153     -14.156     -45.283

REMOVE  C(gr)
  4    2     784.754      -1.324     -10.155     -14.159     -45.133

  4    2     785.047      -1.327     -10.153     -14.158     -45.119


            THEORETICAL ROCKET PERFORMANCE ASSUMING EQUILIBRIUM

          COMPOSITION DURING EXPANSION FROM INFINITE AREA COMBUSTOR

Pin =  1000.0 PSIA
CASE = test2

            REACTANT                    WT FRACTION      ENERGY      TEMP
                                         (SEE NOTE)     KJ/KG-MOL      K
NAME        CH3NO2(L)                    1.0000000   -113100.000    298.000

O/F=    0.00000  %FUEL=  0.000000  R,EQ.RATIO= 1.750000  PHI,EQ.RATIO= 0.000000

                CHAMBER   THROAT     EXIT     EXIT
Pinf/P            1.0000   1.7955   1.0000   675.13
P, BAR            68.947   38.400   68.944  0.10212
T, K             2461.03  2202.73  2461.01   785.05
RHO, KG/CU M    6.8508 0 4.2650 0 6.8506 0 3.2979-2
H, KJ/KG        -1852.88 -2410.45 -1852.93 -5582.93
U, KJ/KG        -2859.30 -3310.78 -2859.33 -5892.59
G, KJ/KG        -30002.9 -27605.9 -30002.7 -14562.5
S, KJ/(KG)(K)    11.4383  11.4383  11.4383  11.4383

M, (1/n)          20.332   20.342   20.332   21.079
MW, MOL WT        20.332   20.342   20.332   21.079
(dLV/dLP)t      -1.00043 -1.00017 -1.00043 -1.04322
(dLV/dLT)p        1.0092   1.0035   1.0092   1.7691
Cp, KJ/(KG)(K)    2.2136   2.1349   2.2136   7.6776
GAMMAs            1.2311   1.2386   1.2311   1.1332
SON VEL,M/SEC     1113.1   1056.0   1113.1    592.4
MACH NUMBER        0.000    1.000    0.008    4.611

PERFORMANCE PARAMETERS

Ae/At                        1.0000   50.000   50.000
CSTAR, M/SEC                 1530.9   1530.9   1530.9
CF                           0.6898   0.0061   1.7842
Ivac, M/SEC                  1908.6 107618.5   2844.7
Isp, M/SEC                   1056.0      9.4   2731.3


MOLE FRACTIONS

CH4              0.00000  0.00000  0.00000  0.01797
*CO              0.27662  0.27188  0.27662  0.10876
*CO2             0.05646  0.06137  0.05646  0.21859
*H               0.00120  0.00044  0.00120  0.00000
HCN              0.00001  0.00000  0.00001  0.00000
```

```
*H2              0.22252  0.22777  0.22252  0.33729
H2O              0.27630  0.27181  0.27630  0.14471
NH3              0.00003  0.00003  0.00003  0.00003
*NO              0.00002  0.00000  0.00002  0.00000
*N2              0.16652  0.16661  0.16652  0.17265
*OH              0.00033  0.00008  0.00033  0.00000

 * THERMODYNAMIC PROPERTIES FITTED TO 20000.K

   PRODUCTS WHICH WERE CONSIDERED BUT WHOSE MOLE FRACTIONS
   WERE LESS THAN 5.000000E-06 FOR ALL ASSIGNED CONDITIONS

*C               *CH              CH2              CH3              CH2OH
CH3O             CH3OH            CH3OOH           *CN              CNN
COOH             *C2              C2H              C2H2,acetylene   C2H2,vinylidene
CH2CO,ketene     O(CH)2O          HO(CO)2OH        C2H3,vinyl       CH3CN
CH3CO,acetyl     C2H4             C2H4O,ethylen-o  CH3CHO,ethanal   CH3COOH
OHCH2COOH        C2H5             C2H6             CH3N2CH3         C2H5OH
CH3OCH3          CH3O2CH3         CCN              CNC              OCCN
C2N2             C2O              *C3              C3H3,1-propynl   C3H3,2-propynl
C3H4,allene      C3H4,propyne     C3H4,cyclo-      C3H5,allyl       C3H6,propylene
C3H6,cyclo-      C3H6O,propylox   C3H6O,acetone    C3H6O,propanal   C3H7,n-propyl
C3H7,i-propyl    C3H8             C3H8O,1propanol  C3H8O,2propanol  CNCOCN
C3O2             *C4              C4H2,butadiyne   C4H4,1,3-cyclo-  C4H6,butadiene
C4H6,1butyne     C4H6,2butyne     C4H6,cyclo-      C4H8,1-butene    C4H8,cis2-buten
C4H8,tr2-butene  C4H8,isobutene   C4H8,cyclo-      (CH3COOH)2       C4H9,n-butyl
C4H9,i-butyl     C4H9,s-butyl     C4H9,t-butyl     C4H10,n-butane   C4H10,isobutane
C4N2             *C5              C5H6,1,3cyclo-   C5H8,cyclo-      C5H10,1-pentene
C5H10,cyclo-     C5H11,pentyl     C5H11,t-pentyl   C5H12,n-pentane  C5H12,i-pentane
CH3C(CH3)2CH3    C6H2             C6H5,phenyl      C6H5O,phenoxy    C6H6
C6H5OH,phenol    C6H10,cyclo-     C6H12,1-hexene   C6H12,cyclo-     C6H13,n-hexyl
C6H14,n-hexane   C7H7,benzyl      C7H8             C7H8O,cresol-mx  C7H14,1-heptene
C7H15,n-heptyl   C7H16,n-heptane  C7H16,2-methylh  C8H8,styrene     C8H10,ethylbenz
C8H16,1-octene   C8H17,n-octyl    C8H18,n-octane   C8H18,isooctane  C9H19,n-nonyl
C10H8,naphthale  C10H21,n-decyl   C12H9,o-bipheny  C12H10,biphenyl  HCO
HCCN             HCCO             HNC              HNCO             HNO
HNO2             HNO3             HO2              HCHO,formaldehy  HCOOH
H2O2             (HCOOH)2         *N               NCO              *NH
NH2              NH2OH            NO2              NO3              NCN
N2H2             NH2NO2           N2H4             N2O              N2O3
N2O4             N2O5             N3               N3H              *O
*O2              O3               C(gr)            H2O(cr)          H2O(L)

NOTE. WEIGHT FRACTION OF FUEL IN TOTAL FUELS AND OF OXIDANT IN TOTAL OXIDANTS

          THEORETICAL ROCKET PERFORMANCE ASSUMING FROZEN COMPOSITION

Pin =  1000.0 PSIA
CASE = test2

            REACTANT                    WT FRACTION      ENERGY      TEMP
                                         (SEE NOTE)     KJ/KG-MOL      K
NAME        CH3NO2(L)                    1.0000000   -113100.000    298.000

O/F=    0.00000  %FUEL=  0.000000  R,EQ.RATIO= 1.750000  PHI,EQ.RATIO= 0.000000

                CHAMBER   THROAT     EXIT     EXIT
Pinf/P            1.0000   1.8003   1.0000   954.94
P, BAR           68.947   38.299   68.944  0.07220
T, K            2461.03  2193.21  2461.01   528.97
RHO, KG/CU M  6.8508 0 4.2702 0 6.8506 0 3.3377-2
H, KJ/KG       -1852.88 -2411.86 -1852.93 -5512.54
U, KJ/KG       -2859.30 -3308.75 -2859.33 -5728.86
```

| | | | | |
|---|---|---|---|---|
| G, KJ/KG | -30002.9 | -27498.4 | -30002.7 | -11563.1 |
| S, KJ/(KG)(K) | 11.4383 | 11.4383 | 11.4383 | 11.4383 |
| M, (1/n) | 20.332 | 20.332 | 20.332 | 20.332 |
| MW, MOL WT | 20.332 | 20.332 | 20.332 | 20.332 |
| Cp, KJ/(KG)(K) | 2.1052 | 2.0678 | 2.1052 | 1.5823 |
| GAMMAs | 1.2411 | 1.2465 | 1.2411 | 1.3485 |
| SON VEL,M/SEC | 1117.6 | 1057.3 | 1117.6 | 540.1 |
| MACH NUMBER | 0.000 | 1.000 | 0.008 | 5.009 |

PERFORMANCE PARAMETERS

| | | | |
|---|---|---|---|
| Ae/At | 1.0000 | 50.000 | 50.000 |
| CSTAR, M/SEC | 1527.1 | 1527.1 | 1527.1 |
| CF | 0.6924 | 0.0061 | 1.7716 |
| Ivac, M/SEC | 1905.6 | 107573.1 | 2785.4 |
| Isp, M/SEC | 1057.3 | 9.4 | 2705.4 |

MOLE FRACTIONS

| | | | | | |
|---|---|---|---|---|---|
| *CO | 0.27662 | *CO2 | 0.05646 | *H | 0.00120 |
| HCN | 0.00001 | *H2 | 0.22252 | H2O | 0.27630 |
| NH3 | 0.00003 | *NO | 0.00002 | *N2 | 0.16652 |
| *OH | 0.00033 | | | | |

* THERMODYNAMIC PROPERTIES FITTED TO 20000.K

PRODUCTS WHICH WERE CONSIDERED BUT WHOSE MOLE FRACTIONS
WERE LESS THAN 5.000000E-06 FOR ALL ASSIGNED CONDITIONS

| | | | | |
|---|---|---|---|---|
| *C | *CH | CH2 | CH3 | CH2OH |
| CH3O | CH3OH | CH3OOH | *CN | CNN |
| COOH | *C2 | C2H | C2H2,acetylene | C2H2,vinylidene |
| CH2CO,ketene | O(CH)2O | HO(CO)2OH | C2H3,vinyl | CH3CN |
| CH3CO,acetyl | C2H4 | C2H4O,ethylen-o | CH3CHO,ethanal | CH3COOH |
| OHCH2COOH | C2H5 | C2H6 | CH3N2CH3 | C2H5OH |
| CH3OCH3 | CH3O2CH3 | CCN | CNC | OCCN |
| C2N2 | C2O | *C3 | C3H3,1-propynl | C3H3,2-propynl |
| C3H4,allene | C3H4,propyne | C3H4,cyclo- | C3H5,allyl | C3H6,propylene |
| C3H6,cyclo- | C3H6O,propylox | C3H6O,acetone | C3H6O,propanal | C3H7,n-propyl |
| C3H7,i-propyl | C3H8 | C3H8O,1propanol | C3H8O,2propanol | CNCOCN |
| C3O2 | *C4 | C4H2,butadiyne | C4H4,1,3-cyclo- | C4H6,butadiene |
| C4H6,1butyne | C4H6,2butyne | C4H6,cyclo- | C4H8,1-butene | C4H8,cis2-buten |
| C4H8,tr2-butene | C4H8,isobutene | C4H8,cyclo- | (CH3COOH)2 | C4H9,n-butyl |
| C4H9,i-butyl | C4H9,s-butyl | C4H9,t-butyl | C4H10,n-butane | C4H10,isobutane |
| C4N2 | *C5 | C5H6,1,3cyclo- | C5H8,cyclo- | C5H10,1-pentene |
| C5H10,cyclo- | C5H11,pentyl | C5H11,t-pentyl | C5H12,n-pentane | C5H12,i-pentane |
| CH3C(CH3)2CH3 | C6H2 | C6H5,phenyl | C6H5O,phenoxy | C6H6 |
| C6H5OH,phenol | C6H10,cyclo- | C6H12,1-hexene | C6H12,cyclo- | C6H13,n-hexyl |
| C6H14,n-hexane | C7H7,benzyl | C7H8 | C7H8O,cresol-mx | C7H14,1-heptene |
| C7H15,n-heptyl | C7H16,n-heptane | C7H16,2-methylh | C8H8,styrene | C8H10,ethylbenz |
| C8H16,1-octene | C8H17,n-octyl | C8H18,n-octane | C8H18,isooctane | C9H19,n-nonyl |
| C10H8,naphthale | C10H21,n-decyl | C12H9,o-bipheny | C12H10,biphenyl | HCO |
| HCCN | HCCO | HNC | HNCO | HNO |
| HNO2 | HNO3 | HO2 | HCHO,formaldehy | HCOOH |
| H2O2 | (HCOOH)2 | *N | NCO | *NH |
| NH2 | NH2OH | NO2 | NO3 | NCN |
| N2H2 | NH2NO2 | N2H4 | N2O | N2O3 |
| N2O4 | N2O5 | N3 | N3H | *O |
| *O2 | O3 | C(gr) | H2O(cr) | H2O(L) |

NOTE. WEIGHT FRACTION OF FUEL IN TOTAL FUELS AND OF OXIDANT IN TOTAL OXIDANTS

# CEA Output for Nitromethane with Stoichiometric Oxygen

```
******************************************************************************

        NASA-GLENN CHEMICAL EQUILIBRIUM PROGRAM CEA2, MAY 21, 2004
                  BY  BONNIE MCBRIDE AND SANFORD GORDON
     REFS: NASA RP-1311, PART I, 1994 AND NASA RP-1311, PART II, 1996

******************************************************************************


problem   case=testox
    rocket  equilibrium  frozen  nfz=1  tcest,k=3000
  p,psia=1000,
  sub,ae/at=50,
  sup,ae/at=50,
react
  fuel=CH3NO2(L) wt=100  t,k=298
  oxid=O2(L) wt=39.3  t,k=90.17
end

OPTIONS: TP=F  HP=F  SP=F  TV=F  UV=F  SV=F  DETN=F  SHOCK=F  REFL=F  INCD=F
RKT=T  FROZ=T  EQL=T  IONS=F  SIUNIT=T  DEBUGF=F  SHKDBG=F  DETDBG=F  TRNSPT=F

TRACE= 0.00E+00  S/R= 0.000000E+00  H/R= 0.000000E+00  U/R= 0.000000E+00

Pc,BAR =    68.947304

Pc/P =

SUBSONIC AREA RATIOS =    50.0000

SUPERSONIC AREA RATIOS =    50.0000

NFZ=  1  Mdot/Ac= 0.000000E+00  Ac/At= 0.000000E+00

   REACTANT          WT.FRAC   (ENERGY/R),K   TEMP,K  DENSITY
       EXPLODED FORMULA
F: CH3NO2(L)        1.000000  -0.136027E+05   298.00  0.0000
         C  1.00000  H  3.00000  N  1.00000  O  2.00000
O: O2(L)            1.000000  -0.156101E+04    90.17  0.0000
         O  2.00000

 SPECIES BEING CONSIDERED IN THIS SYSTEM
(CONDENSED PHASE MAY HAVE NAME LISTED SEVERAL TIMES)
 LAST thermo.inp UPDATE:    9/09/04

 g 7/97  *C               tpis79  *CH              g 4/02  CH2
 g 4/02  CH3              g11/00  CH2OH            g 7/00  CH3O
 g 8/99  CH4              g 7/00  CH3OH           srd 01  CH3OOH
 g 8/99  *CN              g12/99  CNN             tpis79  *CO
 g 9/99  *CO2             tpis91  COOH            tpis91  *C2
 g 6/01  C2H              g 1/91  C2H2,acetylene  g 5/01  C2H2,vinylidene
 g 4/02  CH2CO,ketene     g 3/02  O(CH)2O          srd 01  HO(CO)2OH
 g 7/01  C2H3,vinyl       g 9/00  CH3CN           g 6/96  CH3CO,acetyl
 g 1/00  C2H4             g 8/88  C2H4O,ethylen-o  g 8/88  CH3CHO,ethanal
 g 6/00  CH3COOH          srd 01  OHCH2COOH       g 7/00  C2H5
 g 7/00  C2H6             g 8/88  CH3N2CH3        g 8/88  C2H5OH
 g 7/00  CH3OCH3          srd 01  CH3O2CH3        g 7/00  CCN
 tpis91  CNC              srd 01  OCCN            tpis79  C2N2
 g 8/00  C2O              tpis79  *C3             n 4/98  C3H3,1-propynl
 n 4/98  C3H3,2-propynl   g 2/00  C3H4,allene     g 1/00  C3H4,propyne
```

```
 g 5/90  C3H4,cyclo-      g 3/01  C3H5,allyl       g 2/00  C3H6,propylene
 g 1/00  C3H6,cyclo-      g 6/01  C3H6O,propylox   g 6/97  C3H6O,acetone
 g 1/02  C3H6O,propanal   g 7/01  C3H7,n-propyl    g 9/85  C3H7,i-propyl
 g 2/00  C3H8             g 2/00  C3H8O,1propanol  g 2/00  C3H8O,2propanol
 srd 01  CNCOCN           g 7/88  C3O2             g tpis  *C4
 g 7/01  C4H2,butadiyne   g 8/00  C4H4,1,3-cyclo-  n10/92  C4H6,butadiene
 n10/93  C4H6,1butyne     n10/93  C4H6,2butyne     g 8/00  C4H6,cyclo-
 n 4/88  C4H8,1-butene    n 4/88  C4H8,cis2-buten  n 4/88  C4H8,tr2-butene
 n 4/88  C4H8,isobutene   g 8/00  C4H8,cyclo-      g10/00  (CH3COOH)2
 n10/84  C4H9,n-butyl     n10/84  C4H9,i-butyl     g 1/93  C4H9,s-butyl
 g 1/93  C4H9,t-butyl     g12/00  C4H10,n-butane   g 8/00  C4H10,isobutane
 g 6/01  C4N2             g 8/00  *C5              g 5/90  C5H6,1,3cyclo-
 g 1/93  C5H8,cyclo-      n 4/87  C5H10,1-pentene  g 2/01  C5H10,cyclo-
 n10/84  C5H11,pentyl     g 1/93  C5H11,t-pentyl   n10/85  C5H12,n-pentane
 n10/85  C5H12,i-pentane  n10/85  CH3C(CH3)2CH3    g 2/93  C6H2
 g11/00  C6H5,phenyl      g 8/00  C6H5O,phenoxy    g 8/00  C6H6
 g 8/00  C6H5OH,phenol    g 1/93  C6H10,cyclo-     n 4/87  C6H12,1-hexene
 g 6/90  C6H12,cyclo-     n10/83  C6H13,n-hexyl    g 6/01  C6H14,n-hexane
 g 7/01  C7H7,benzyl      g 1/93  C7H8             g12/00  C7H8O,cresol-mx
 n 4/87  C7H14,1-heptene  n10/83  C7H15,n-heptyl   n10/85  C7H16,n-heptane
 n10/85  C7H16,2-methylh  n 4/89  C8H8,styrene     n10/86  C8H10,ethylbenz
 n 4/87  C8H16,1-octene   n10/83  C8H17,n-octyl    n 4/85  C8H18,n-octane
 n 4/85  C8H18,isooctane  n10/83  C9H19,n-nonyl    g 3/01  C10H8,naphthale
 n10/83  C10H21,n-decyl   g 8/00  C12H9,o-bipheny  g 8/00  C12H10,biphenyl
 g 6/97  *H               g 6/01  HCN              g 1/01  HCO
 tpis89  HCCN             g 6/01  HCCO             g 6/01  HNC
 g 7/00  HNCO             g10/01  HNO              tpis89  HNO2
 g 5/99  HNO3             g 4/02  HO2              tpis78  *H2
 g 5/01  HCHO,formaldehy  g 6/01  HCOOH           g 8/89  H2O
 g 6/99  H2O2             g 6/01  (HCOOH)2         g 5/97  *N
 g 6/01  NCO              g 4/99  *NH             g 3/01  NH2
 tpis89  NH3              tpis89  NH2OH           tpis89  *NO
 g 4/99  NO2              j12/64  NO3              tpis78  *N2
 g 6/01  NCN              g 5/99  N2H2            tpis89  NH2NO2
 g 4/99  N2H4             g 4/99  N2O             g 4/99  N2O3
 tpis89  N2O4             g 4/99  N2O5            tpis89  N3
 g 4/99  N3H              g 5/97  *O              g 4/02  *OH
 tpis89  *O2              g 8/01  O3              n 4/83  C(gr)
 n 4/83  C(gr)            n 4/83  C(gr)           g11/99  H2O(cr)
 g 8/01  H2O(L)           g 8/01  H2O(L)

O/F =   0.393000

                        EFFECTIVE FUEL     EFFECTIVE OXIDANT        MIXTURE
ENTHALPY                    h(2)/R             h(1)/R               h0/R
(KG-MOL)(K)/KG       -0.22284930E+03    -0.48783267E+02    -0.17374094E+03

KG-FORM.WT./KG             bi(2)              bi(1)              b0i
 *C                  0.16382695E-01     0.00000000E+00     0.11760728E-01
 *H                  0.49148084E-01     0.00000000E+00     0.35282185E-01
 *N                  0.16382695E-01     0.00000000E+00     0.11760728E-01
 *O                  0.32765389E-01     0.62502344E-01     0.41154925E-01

POINT ITN      T            C           H           N           O

  1   22    3375.233     -16.702     -10.281     -13.268     -14.779

Pinf/Pt = 1.727204
  2    3    3213.973     -17.150     -10.519     -13.438     -14.990

Pinf/Pt = 1.725099
  2    2    3214.321     -17.149     -10.519     -13.438     -14.989
```

| | | | | | | |
|---|---|---|---|---|---|---|
| 3 | 1 | 3375.228 | -16.702 | -10.281 | -13.268 | -14.779 |
| 3 | 1 | 3375.221 | -16.702 | -10.281 | -13.268 | -14.779 |
| 4 | 6 | 1754.613 | -24.488 | -14.037 | -15.335 | -18.480 |
| 4 | 4 | 1865.145 | -23.599 | -13.658 | -15.213 | -18.069 |
| 4 | 2 | 1864.905 | -23.601 | -13.659 | -15.214 | -18.070 |

THEORETICAL ROCKET PERFORMANCE ASSUMING EQUILIBRIUM

COMPOSITION DURING EXPANSION FROM INFINITE AREA COMBUSTOR

Pin = 1000.0 PSIA
CASE = testox

| | REACTANT | WT FRACTION (SEE NOTE) | ENERGY KJ/KG-MOL | TEMP K |
|---|---|---|---|---|
| FUEL | CH3NO2(L) | 1.0000000 | -113100.000 | 298.000 |
| OXIDANT | O2(L) | 1.0000000 | -12979.000 | 90.170 |

O/F= 0.39300 %FUEL= 71.787509 R,EQ.RATIO= 1.000185 PHI,EQ.RATIO= 1.000432

| | CHAMBER | THROAT | EXIT | EXIT |
|---|---|---|---|---|
| Pinf/P | 1.0000 | 1.7251 | 1.0000 | 471.48 |
| P, BAR | 68.947 | 39.967 | 68.945 | 0.14624 |
| T, K | 3375.23 | 3214.32 | 3375.22 | 1864.90 |
| RHO, KG/CU M | 6.2875 0 | 3.8738 0 | 6.2873 0 | 2.6616-2 |
| H, KJ/KG | -1444.57 | -2024.59 | -1444.62 | -6359.47 |
| U, KJ/KG | -2541.15 | -3056.31 | -2541.19 | -6908.91 |
| G, KJ/KG | -37140.0 | -36018.3 | -37140.0 | -26082.2 |
| S, KJ/(KG)(K) | 10.5757 | 10.5757 | 10.5757 | 10.5757 |
| M, (1/n) | 25.592 | 25.904 | 25.592 | 28.221 |
| (dLV/dLP)t | -1.03044 | -1.02729 | -1.03044 | -1.00146 |
| (dLV/dLT)p | 1.5861 | 1.5535 | 1.5861 | 1.0520 |
| Cp, KJ/(KG)(K) | 5.6954 | 5.6166 | 5.6954 | 2.3596 |
| GAMMAs | 1.1275 | 1.1244 | 1.1275 | 1.1584 |
| SON VEL,M/SEC | 1111.9 | 1077.1 | 1111.9 | 797.8 |
| MACH NUMBER | 0.000 | 1.000 | 0.008 | 3.930 |

PERFORMANCE PARAMETERS

| | | | |
|---|---|---|---|
| Ae/At | 1.0000 | 50.000 | 50.000 |
| CSTAR, M/SEC | 1652.5 | 1652.5 | 1652.5 |
| CF | 0.6518 | 0.0057 | 1.8973 |
| Ivac, M/SEC | 2035.0 | 116530.7 | 3310.5 |
| Isp, M/SEC | 1077.1 | 9.4 | 3135.3 |

MOLE FRACTIONS

| | | | | |
|---|---|---|---|---|
| *CO | 0.11420 | 0.10325 | 0.11420 | 0.00579 |
| *CO2 | 0.18676 | 0.20139 | 0.18676 | 0.32611 |
| COOH | 0.00001 | 0.00001 | 0.00001 | 0.00000 |
| *H | 0.00912 | 0.00752 | 0.00912 | 0.00007 |
| HNO | 0.00001 | 0.00001 | 0.00001 | 0.00000 |
| HO2 | 0.00015 | 0.00010 | 0.00015 | 0.00000 |
| *H2 | 0.02946 | 0.02643 | 0.02946 | 0.00216 |
| H2O | 0.38959 | 0.40279 | 0.38959 | 0.49492 |
| H2O2 | 0.00002 | 0.00001 | 0.00002 | 0.00000 |
| *N | 0.00001 | 0.00000 | 0.00001 | 0.00000 |

| | | | | |
|---|---|---|---|---|
| *NO | 0.01458 | 0.01210 | 0.01458 | 0.00030 |
| NO2 | 0.00003 | 0.00002 | 0.00003 | 0.00000 |
| *N2 | 0.14317 | 0.14625 | 0.14317 | 0.16580 |
| *O | 0.00938 | 0.00752 | 0.00938 | 0.00003 |
| *OH | 0.05549 | 0.04783 | 0.05549 | 0.00147 |
| *O2 | 0.04801 | 0.04475 | 0.04801 | 0.00335 |

* THERMODYNAMIC PROPERTIES FITTED TO 20000.K

PRODUCTS WHICH WERE CONSIDERED BUT WHOSE MOLE FRACTIONS
WERE LESS THAN 5.000000E-06 FOR ALL ASSIGNED CONDITIONS

| | | | | |
|---|---|---|---|---|
| *C | *CH | CH2 | CH3 | CH2OH |
| CH3O | CH4 | CH3OH | CH3OOH | *CN |
| CNN | *C2 | C2H | C2H2,acetylene | C2H2,vinylidene |
| CH2CO,ketene | O(CH)2O | HO(CO)2OH | C2H3,vinyl | CH3CN |
| CH3CO,acetyl | C2H4 | C2H4O,ethylen-o | CH3CHO,ethanal | CH3COOH |
| OHCH2COOH | C2H5 | C2H6 | CH3N2CH3 | C2H5OH |
| CH3OCH3 | CH3O2CH3 | CCN | CNC | OCCN |
| C2N2 | C2O | *C3 | C3H3,1-propynl | C3H3,2-propynl |
| C3H4,allene | C3H4,propyne | C3H4,cyclo- | C3H5,allyl | C3H6,propylene |
| C3H6,cyclo- | C3H6O,propylox | C3H6O,acetone | C3H6O,propanal | C3H7,n-propyl |
| C3H7,i-propyl | C3H8 | C3H8O,1propanol | C3H8O,2propanol | CNCOCN |
| C3O2 | *C4 | C4H2,butadiyne | C4H4,1,3-cyclo- | C4H6,butadiene |
| C4H6,1butyne | C4H6,2butyne | C4H6,cyclo- | C4H8,1-butene | C4H8,cis2-buten |
| C4H8,tr2-butene | C4H8,isobutene | C4H8,cyclo- | (CH3COOH)2 | C4H9,n-butyl |
| C4H9,i-butyl | C4H9,s-butyl | C4H9,t-butyl | C4H10,n-butane | C4H10,isobutane |
| C4N2 | *C5 | C5H6,1,3cyclo- | C5H8,cyclo- | C5H10,1-pentene |
| C5H10,cyclo- | C5H11,pentyl | C5H11,t-pentyl | C5H12,n-pentane | C5H12,i-pentane |
| CH3C(CH3)2CH3 | C6H2 | C6H5,phenyl | C6H5O,phenoxy | C6H6 |
| C6H5OH,phenol | C6H10,cyclo- | C6H12,1-hexene | C6H12,cyclo- | C6H13,n-hexyl |
| C6H14,n-hexane | C7H7,benzyl | C7H8 | C7H8O,cresol-mx | C7H14,1-heptene |
| C7H15,n-heptyl | C7H16,n-heptane | C7H16,2-methylh | C8H8,styrene | C8H10,ethylbenz |
| C8H16,1-octene | C8H17,n-octyl | C8H18,n-octane | C8H18,isooctane | C9H19,n-nonyl |
| C10H8,naphthale | C10H21,n-decyl | C12H9,o-bipheny | C12H10,biphenyl | HCN |
| HCO | HCCN | HCCO | HNC | HNCO |
| HNO2 | HNO3 | HCHO,formaldehy | HCOOH | (HCOOH)2 |
| NCO | *NH | NH2 | NH3 | NH2OH |
| NO3 | NCN | N2H2 | NH2NO2 | N2H4 |
| N2O | N2O3 | N2O4 | N2O5 | N3 |
| N3H | O3 | C(gr) | H2O(cr) | H2O(L) |

NOTE. WEIGHT FRACTION OF FUEL IN TOTAL FUELS AND OF OXIDANT IN TOTAL OXIDANTS

THEORETICAL ROCKET PERFORMANCE ASSUMING FROZEN COMPOSITION

Pin = 1000.0 PSIA
CASE = testox

| | REACTANT | WT FRACTION (SEE NOTE) | ENERGY KJ/KG-MOL | TEMP K |
|---|---|---|---|---|
| FUEL | CH3NO2(L) | 1.0000000 | -113100.000 | 298.000 |
| OXIDANT | O2(L) | 1.0000000 | -12979.000 | 90.170 |

O/F= 0.39300 %FUEL= 71.787509 R,EQ.RATIO= 1.000185 PHI,EQ.RATIO= 1.000432

| | CHAMBER | THROAT | EXIT | EXIT |
|---|---|---|---|---|
| Pinf/P | 1.0000 | 1.7731 | 1.0000 | 717.15 |
| P, BAR | 68.947 | 38.886 | 68.944 | 0.09614 |
| T, K | 3375.23 | 3066.93 | 3375.21 | 1014.20 |
| RHO, KG/CU M | 6.2875 0 | 3.9026 0 | 6.2873 0 | 2.9178-2 |
| H, KJ/KG | -1444.57 | -2043.50 | -1444.62 | -5730.47 |
| U, KJ/KG | -2541.15 | -3039.92 | -2541.19 | -6059.97 |

| | | | | |
|---|---|---|---|---|
| G, KJ/KG | -37140.0 | -34478.4 | -37139.8 | -16456.4 |
| S, KJ/(KG)(K) | 10.5757 | 10.5757 | 10.5757 | 10.5757 |
| M, (1/n) | 25.592 | 25.592 | 25.592 | 25.592 |
| Cp, KJ/(KG)(K) | 1.9528 | 1.9319 | 1.9528 | 1.5627 |
| GAMMAs | 1.1996 | 1.2022 | 1.1996 | 1.2625 |
| SON VEL,M/SEC | 1146.9 | 1094.5 | 1146.9 | 645.0 |
| MACH NUMBER | 0.000 | 1.000 | 0.008 | 4.539 |

PERFORMANCE PARAMETERS

| | | | |
|---|---|---|---|
| Ae/At | 1.0000 | 50.000 | 50.000 |
| CSTAR, M/SEC | 1614.2 | 1614.2 | 1614.2 |
| CF | 0.6780 | 0.0060 | 1.8137 |
| Ivac, M/SEC | 2004.9 | 113748.6 | 3040.3 |
| Isp, M/SEC | 1094.5 | 9.6 | 2927.8 |

MOLE FRACTIONS

| | | | | | |
|---|---|---|---|---|---|
| *CO | 0.11420 | *CO2 | 0.18676 | COOH | 0.00001 |
| *H | 0.00912 | HNO | 0.00001 | HO2 | 0.00015 |
| *H2 | 0.02946 | H2O | 0.38959 | H2O2 | 0.00002 |
| *N | 0.00001 | *NO | 0.01458 | NO2 | 0.00003 |
| *N2 | 0.14317 | *O | 0.00938 | *OH | 0.05549 |
| *O2 | 0.04801 | | | | |

* THERMODYNAMIC PROPERTIES FITTED TO 20000.K

PRODUCTS WHICH WERE CONSIDERED BUT WHOSE MOLE FRACTIONS
WERE LESS THAN 5.000000E-06 FOR ALL ASSIGNED CONDITIONS

| | | | | |
|---|---|---|---|---|
| *C | *CH | CH2 | CH3 | CH2OH |
| CH3O | CH4 | CH3OH | CH3OOH | *CN |
| CNN | *C2 | C2H | C2H2,acetylene | C2H2,vinylidene |
| CH2CO,ketene | O(CH)2O | HO(CO)2OH | C2H3,vinyl | CH3CN |
| CH3CO,acetyl | C2H4 | C2H4O,ethylen-o | CH3CHO,ethanal | CH3COOH |
| OHCH2COOH | C2H5 | C2H6 | CH3N2CH3 | C2H5OH |
| CH3OCH3 | CH3O2CH3 | CCN | CNC | OCCN |
| C2N2 | C2O | *C3 | C3H3,1-propynl | C3H3,2-propynl |
| C3H4,allene | C3H4,propyne | C3H4,cyclo- | C3H5,allyl | C3H6,propylene |
| C3H6,cyclo- | C3H6O,propylox | C3H6O,acetone | C3H6O,propanal | C3H7,n-propyl |
| C3H7,i-propyl | C3H8 | C3H8O,1propanol | C3H8O,2propanol | CNCOCN |
| C3O2 | *C4 | C4H2,butadiyne | C4H4,1,3-cyclo- | C4H6,butadiene |
| C4H6,1butyne | C4H6,2butyne | C4H6,cyclo- | C4H8,1-butene | C4H8,cis2-buten |
| C4H8,tr2-butene | C4H8,isobutene | C4H8,cyclo- | (CH3COOH)2 | C4H9,n-butyl |
| C4H9,i-butyl | C4H9,s-butyl | C4H9,t-butyl | C4H10,n-butane | C4H10,isobutane |
| C4N2 | *C5 | C5H6,1,3cyclo- | C5H8,cyclo- | C5H10,1-pentene |
| C5H10,cyclo- | C5H11,pentyl | C5H11,t-pentyl | C5H12,n-pentane | C5H12,i-pentane |
| CH3C(CH3)2CH3 | C6H2 | C6H5,phenyl | C6H5O,phenoxy | C6H6 |
| C6H5OH,phenol | C6H10,cyclo- | C6H12,1-hexene | C6H12,cyclo- | C6H13,n-hexyl |
| C6H14,n-hexane | C7H7,benzyl | C7H8 | C7H8O,cresol-mx | C7H14,1-heptene |
| C7H15,n-heptyl | C7H16,n-heptane | C7H16,2-methylh | C8H8,styrene | C8H10,ethylbenz |
| C8H16,1-octene | C8H17,n-octyl | C8H18,n-octane | C8H18,isooctane | C9H19,n-nonyl |
| C10H8,naphthale | C10H21,n-decyl | C12H9,o-bipheny | C12H10,biphenyl | HCN |
| HCO | HCCN | HCCO | HNC | HNCO |
| HNO2 | HNO3 | HCHO,formaldehy | HCOOH | (HCOOH)2 |
| NCO | *NH | NH2 | NH3 | NH2OH |
| NO3 | NCN | N2H2 | NH2NO2 | N2H4 |
| N2O | N2O3 | N2O4 | N2O5 | N3 |
| N3H | O3 | C(gr) | H2O(cr) | H2O(L) |

NOTE. WEIGHT FRACTION OF FUEL IN TOTAL FUELS AND OF OXIDANT IN TOTAL OXIDANTS

# VITA


Name: William Charles Warren

Address: Department of Mechanical Engineering
3123 TAMU
College Station, Texas 77843-3123

Email Address: william.c.warren@tamu.edu
william.c.warren@gmail.com


Education: B.S. Mechanical Engineering, with honors
Minor in Mathematics
The University of Alabama, 2010

M.S. Mechanical Engineering
Texas A&M University, 2012